2021-06

A MANUFACTURING PROCESS TO IMPLEMENT TRANSONIC COMPRESSOR ENDWALL CASING TREATMENT

Green, Jeremy C.

Monterey, CA; Naval Postgraduate School

NAVAL POSTGRADUATE SCHOOL

MONTEREY, CALIFORNIA

THESIS

A MANUFACTURING PROCESS TO IMPLEMENT TRANSONIC COMPRESSOR ENDWALL CASING TREATMENTS

by

Jeremy C. Green

June 2021

Thesis Advisor: Anthony J. Gannon
Co-Advisor: Walter Smith

THIS PAGE INTENTIONALLY LEFT BLANK

REPORT DOCUMENTATION PAGE			*Form Approved OMB No. 0704-0188*

1. AGENCY USE ONLY *(Leave blank)*	**2. REPORT DATE** June 2021	**3. REPORT TYPE AND DATES COVERED** Master's thesis

4. TITLE AND SUBTITLE A MANUFACTURING PROCESS TO IMPLEMENT TRANSONIC COMPRESSOR ENDWALL CASING TREATMENTS	**5. FUNDING NUMBERS** RMNPB
6. AUTHOR(S) Jeremy C. Green	
7. PERFORMING ORGANIZATION NAME(S) AND ADDRESS(ES) Naval Postgraduate School Monterey, CA 93943-5000	**8. PERFORMING ORGANIZATION REPORT NUMBER**
9. SPONSORING / MONITORING AGENCY NAME(S) AND ADDRESS(ES) Office of Naval Research Monterey, CA, 93943	**10. SPONSORING / MONITORING AGENCY REPORT NUMBER**

11. SUPPLEMENTARY NOTES The views expressed in this thesis are those of the author and do not reflect the official policy or position of the Department of Defense or the U.S. Government.

12a. DISTRIBUTION / AVAILABILITY STATEMENT Approved for public release. Distribution is unlimited.	**12b. DISTRIBUTION CODE** A

13. ABSTRACT (maximum 200 words)

The goal of this thesis is to create a manufacturing process that will be used to implement transonic compressor treatments in the form of grooves or passages beneath the endwall surface. The main goal of the treatments are to extend the stability margin of the gas turbine engine without significantly harming its efficiency. This is done by redirecting flow to the axial direction near stall or by hindering the formation of harmful flow features such as the tip leakage vortex. The specific geometries of the treatments are based on empirical and experimental data previously collected in other studies. Implementing treatments was done by casting the desired geometry into a layer of epoxy on the endwall surface, using molds and attachments made by additive manufacturing. It was found that using water soluble molds was a necessary feature of surface treatment molds in epoxy. The same material was used to mold internal passages that would be used to recirculate high pressure air from behind the rotor to the low pressure region upstream of the rotor. Fanno flow calculations provided a way to determine the mass flow rate through a single passage, and therefore how many passages of a specific size and shape would be needed to recirculate a certain percentage of mass flow through the compressor. By keeping the passages within the epoxy layer, the inner diameter of the casing was only increased by about 2 percent.

14. SUBJECT TERMS transonic compressor treatments, tip leakage vortex, manufacturing process	**15. NUMBER OF PAGES** 95
	16. PRICE CODE

17. SECURITY CLASSIFICATION OF REPORT	**18. SECURITY CLASSIFICATION OF THIS PAGE**	**19. SECURITY CLASSIFICATION OF ABSTRACT**	**20. LIMITATION OF ABSTRACT**
Unclassified	Unclassified	Unclassified	UU

NSN 7540-01-280-5500

Standard Form 298 (Rev. 2-89)
Prescribed by ANSI Std. 239-18

THIS PAGE INTENTIONALLY LEFT BLANK

Approved for public release. Distribution is unlimited.

A MANUFACTURING PROCESS TO IMPLEMENT TRANSONIC COMPRESSOR ENDWALL CASING TREATMENTS

Jeremy C. Green
Ensign, United States Navy
BSME, The Citadel, 2020

Submitted in partial fulfillment of the
requirements for the degree of

**MASTER OF SCIENCE IN ENGINEERING SCIENCE
(AEROSPACE ENGINEERING)**

from the

**NAVAL POSTGRADUATE SCHOOL
June 2021**

Approved by: Anthony J. Gannon
Advisor

Walter Smith
Co-Advisor

Garth V. Hobson
Chair, Department of Mechanical and Aerospace Engineering

THIS PAGE INTENTIONALLY LEFT BLANK

ABSTRACT

The goal of this thesis is to create a manufacturing process that will be used to implement transonic compressor treatments in the form of grooves or passages beneath the endwall surface. The main goal of the treatments are to extend the stability margin of the gas turbine engine without significantly harming its efficiency. This is done by redirecting flow to the axial direction near stall or by hindering the formation of harmful flow features such as the tip leakage vortex. The specific geometries of the treatments are based on empirical and experimental data previously collected in other studies. Implementing treatments was done by casting the desired geometry into a layer of epoxy on the endwall surface, using molds and attachments made by additive manufacturing. It was found that using water soluble molds was a necessary feature of surface treatment molds in epoxy. The same material was used to mold internal passages that would be used to recirculate high pressure air from behind the rotor to the low pressure region upstream of the rotor. Fanno flow calculations provided a way to determine the mass flow rate through a single passage, and therefore how many passages of a specific size and shape would be needed to recirculate a certain percentage of mass flow through the compressor. By keeping the passages within the epoxy layer, the inner diameter of the casing was only increased by about 2 percent.

THIS PAGE INTENTIONALLY LEFT BLANK

TABLE OF CONTENTS

THIS PAGE INTENTIONALLY LEFT BLANK

LIST OF FIGURES

THIS PAGE INTENTIONALLY LEFT BLANK

LIST OF TABLES

THIS PAGE INTENTIONALLY LEFT BLANK

LIST OF ACRONYMS AND ABBREVIATIONS

NPS	Naval Postgraduate School
PLA	Polylactic Acid (3D printer filament used throughout study)
PS	Pressure Side
PVA	Polyvinyl Alcohol (3D printer support material)
SS	Suction Side
TCR	Transonic Compressor Test Rig
TLV	Tip Leakage Vortex
μ	Dynamic Viscosity of Air, 1.79E-5 Ns/m^2
ρ	Density of Air, 1.255 kg/m^3
γ	Ratio of Specific Heats of Air, 1.4
R	Specific Gas Constant of Air, 287 J/kgK

THIS PAGE INTENTIONALLY LEFT BLANK

I. INTRODUCTION

A. COMPRESSOR STAGE OF AN AXIAL TURBOMACHINE

Gas turbine engines are present in multiple communities across the Navy. They provide thrust or a means of propulsion for many aircraft and ships. They also tend to be more efficient than the well-known diesel or combustion engine. In aircraft, gas turbine engines provide thrust by compressing, combusting, and expelling accelerated air through a nozzle. For a similar mass of air entering and exiting the engine, being able to accelerate the exiting air means that that an equal force must push the engine forward. Gas turbine engines can also create shaft power to provide propulsion for a ship's screw. This is done by passing the combusted air through a turbine that can deliver the rotational motion to the ship's propulsion shaft. Figure 1 shows a cross section of a typical gas turbine engine.

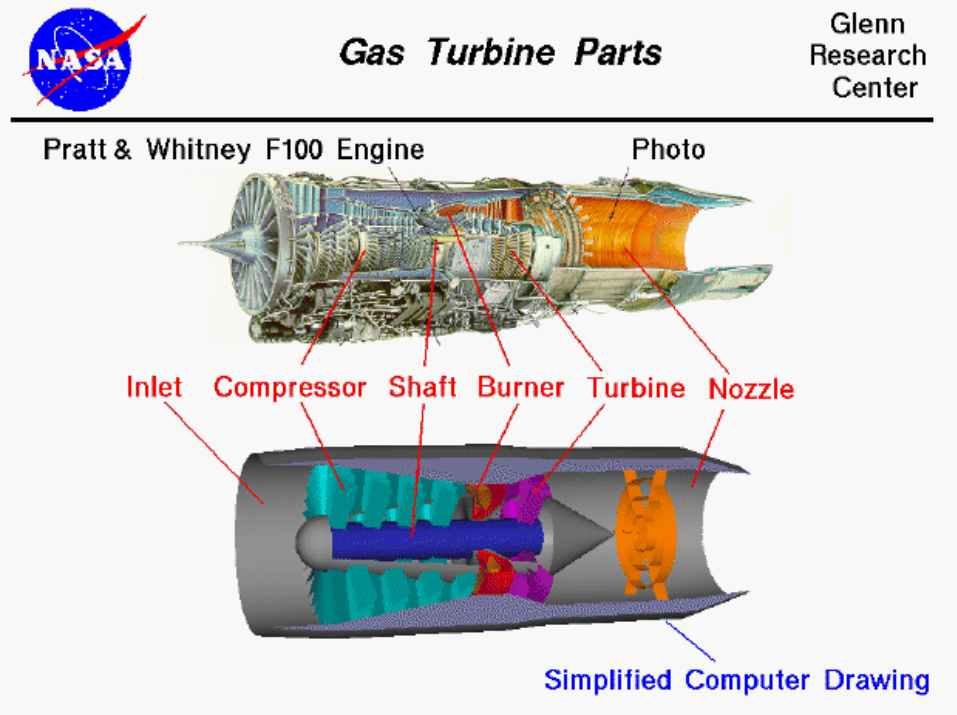

Figure 1. Gas Turbine Engine Schematic. Source: [1].

The incoming fluid flow encounters the first stage when entering a compressor of a turbomachine. Figure 2 shows the cross section of a compressor to illustrate the typical sequence of components.

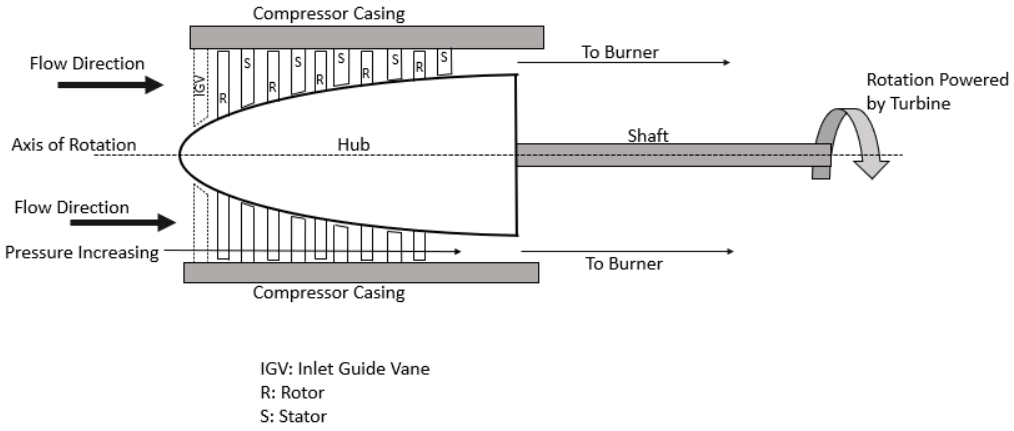

Figure 2. Axial Compressor Cross Section

The compressor's main purpose is to compress the air for expansion through combustion, which will in turn drive the turbine and provide thrust for the engine in the later stages. It is physically a large portion of the machine as a whole, and can have a number of different stages within it. The main components of the compressor stage in order from front to rear can include inlet guide vanes and an alternating pattern of rotors and stators. The inlet guide vane serves to guide the flow into the first rotor at a more favorable angle. The rotors are attached to a hub located at the center of the compressor that rotates on a shaft powered by the turbine stage of the engine. The stators are fixed blades that are attached to the casing wall, and serve to redirect the flow angle for the following rotor stage. With each stage the air passes through, pressure is increased to allow for combustion following the compressor stage. However, gas turbine engines are often limited in operability by the onset of compressor stall. When stalling occurs, air is not able to cross the compressor rotor passages to get to the burner or turbine. Without air flowing through the engine, no thrust or propulsion can be provided to the aircraft or ship. By extending the stall margin of the compressor, one may therefore extend the operating envelope of the

ship or aircraft. For this study, inlet guide vanes were not included. The compressor casing wall and how to modify the fluid behavior between it and the rotor blade tip are the main focus of this study.

B. LITERATURE REVIEW

A rotor blade in an axial turbomachine will generate high pressure on the side facing the direction of rotation and low pressure on the side facing opposite the direction of rotation. See Figure 3 for reference. The difference in pressure causes flow to move in the tip clearance region between the blade tip and compressor wall from the pressure side, (PS), to the suction side, (SS). When this happens, the flow rolls up to form a vortex at the blade tip known as a tip leakage vortex (TLV). This behavior is similar to the vortices on the leading edge of a delta wing, only much smaller in size [2, 3]. Figure 3 and Figure 4 show TLVs from experimental studies in the form of photographs and ensemble averaged velocity components taken with particle image velocimetry respectively.

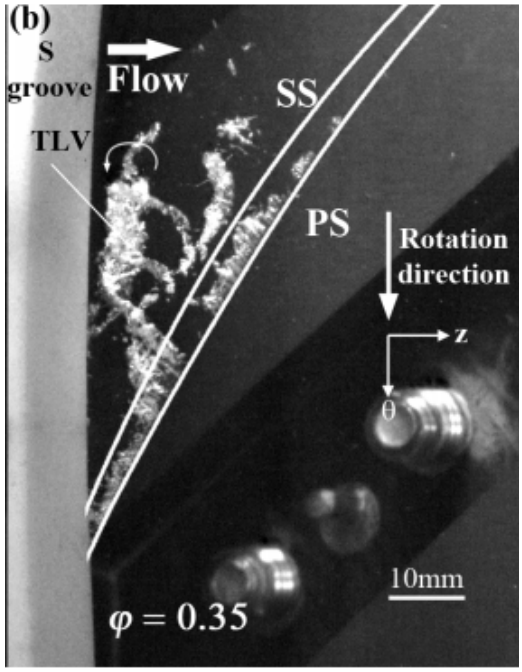

Figure 3. Tip Leakage Vortices Behind a Rotor Blade Passing Over S-Groove Casing Treatment. Adapted from [4]

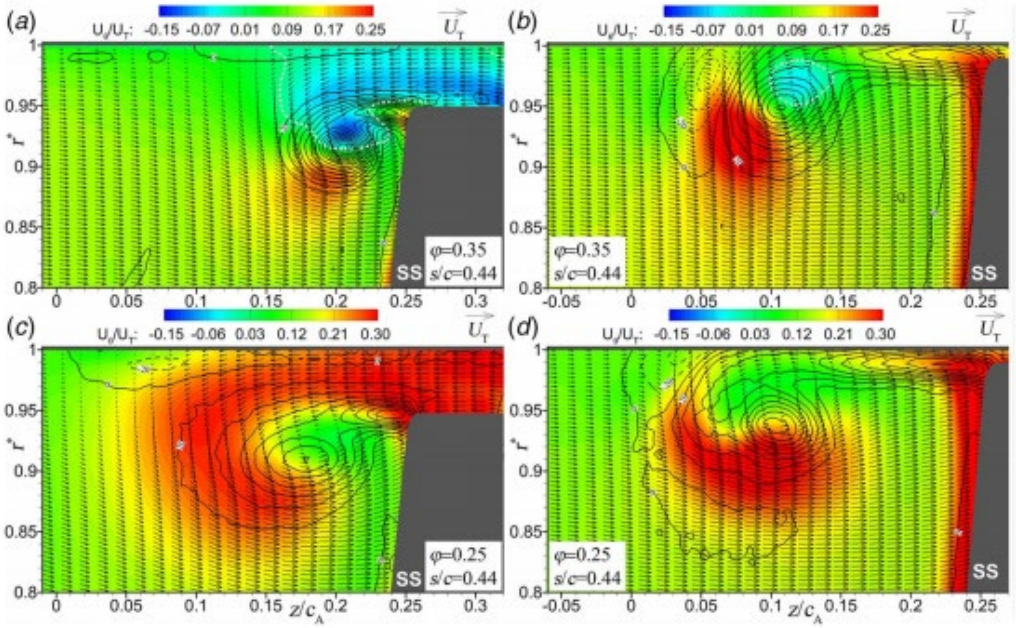

Figure 4. Tip Leakage Vortex Visualization. Source: [3]

The TLV is a detrimental flow feature in turbomachinery because it can cause flow blockage at the endwall, which leads to performance losses, stall, and even cavitation in axial water pumps [5]. The exact reasons for these phenomena are not fully understood. Some studies suggest that the TLV expansion in the downstream direction causes blockage by drastically altering flow fields out of the axial plane, which gives rise to low-energy fluid motion, boundary layer separation on the suction side of the blade, and a drop in the pressure ratio across the rotor [2]. TLVs are not the sole cause of stall, but do seem to expedite it. Tests have shown that TLVs tend to disappear and are replaced by a secondary flow in the radial direction near the stall condition [2]. Figure 5 shows velocity vectors measured by a hot wire just downstream of an axial compressor rotor at design conditions and near stall conditions for the purpose of comparison.

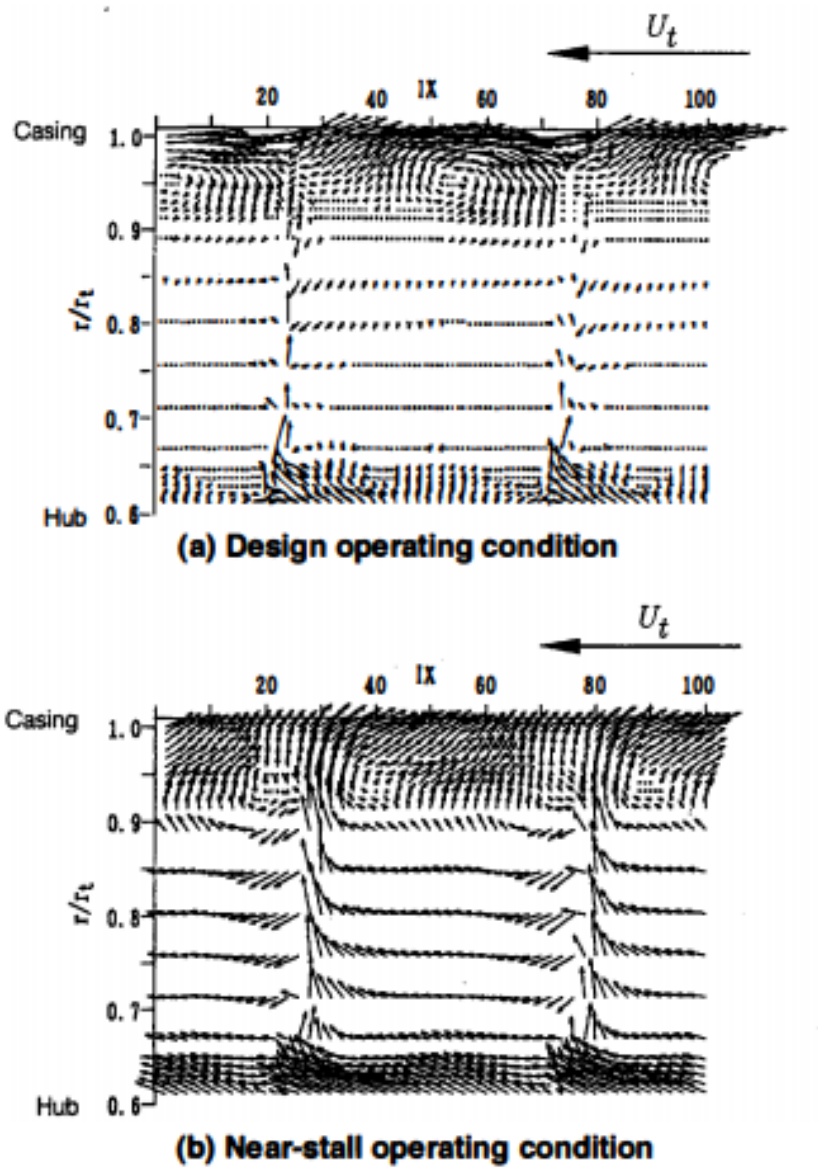

Figure 5. Secondary Flow Vectors Downstream of the Rotor Passage.
Source: [2]

The velocity vectors in the near-stall operating condition display a much stronger flow in the radial direction. It is known that endwall treatments can have an appreciable effect on delaying compressor stall. Although the flow interactions that make a treatment successful are not exactly understood yet, it is known that the quality and uniformity of the flow in the tip clearance region will aid in the stability of the gas turbine and increase the stall margin. Some theories suggest that the treatment's role in recirculating nonuniform or

distorted flow increases flow uniformity downstream of the compressor rotor blades [6]. Some casing treatments are aimed to diminish the TLV size and strength by capturing it or creating a vortex of opposite vorticity to counter it [4]. Other treatments recirculate flow from the high-pressure region aft of the rotor to the low-pressure region upstream of the rotor to direct more flow to the axial direction and decrease the pressure difference in the blade passage, (from the PS to the SS), near stall [6,7]. Some casing treatments have taken the form of axial slots, circumferential slots, and derivatives of the like, that provide a base for studying endwall treatment effects on performance. Most of these grooves and slots are made by cutting into the casing wall while spinning, or cutting straight lines in the axial direction.

With the advancement of casing treatments over time, another form of casing treatment has emerged. Rather than redirect flow along the face of the casing wall, some redirect flow outside the casing in the form of tubular passages [6,7]. While much more complex and difficult to manufacture, this treatment form tends to show higher performance gains due to its ability to redirect more flow. However, recirculating flow that has been worked already will intuitively lead to losses in efficiency because the rotor has to perform more work on the same net mass flow into the compressor. This trade off of stall margin improvement and efficiency loss has been the traditional struggle of compressor casing treatment design.

C. MOTIVATION

This casing treatment study is split into two parts: surface treatments and internal passages. The work of this study is to create a manufacturing process that can be used to implement either type of treatment. The specific concepts, geometries, and methods that were the inspiration for each type of treatment will be discussed in the treatment's respective chapter. To reiterate, by implementing a treatment that extends the stall margin of the compressor, the operating range of the engine could also be extended. Therefore, the aim of this study is to provide a manufacturing process that can be used to test and study different casing treatments for an axial compressor casing for the purpose of stall margin increase.

II. DESIGN OF THE SURFACE CASING TREATMENTS

A. BACKGROUND

In the case of surface treatments, of specific interest are several geometries modeled by Chen et al. [4]. in March of 2020. Their proposed casing treatments are reported to delay compressor stall while avoiding a sizeable efficiency penalty. They are described as the U-shape groove and the S-shape groove, respectively. Their shapes and dimensions are shown in Figure 6.

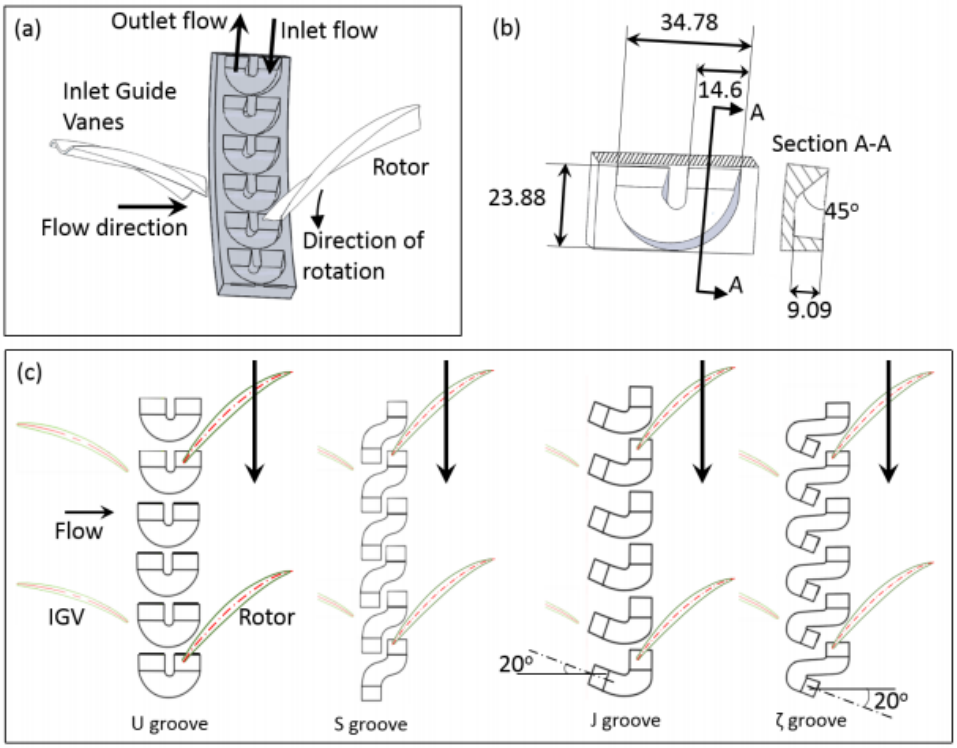

Figure 6. Casing Treatment Grooves Tested by Chen et al. Source: [5]

The J and ζ grooves were omitted in this study mostly because the manufacturing process would be similar as that for the U and S-grooves, and they achieved lesser success. Testing these grooves in a low-speed axial compressor with water as the working fluid showed that the U-grooves would provide a 60% stall margin improvement while only

incurring a 2% loss in efficiency. The same study also yielded that the S-grooves would provide a 36% stall margin improvement and little to no efficiency penalty [4]. Figure 7 plots the performance and efficiency curves for each of the treatments shown in Figure 6, as well as a smooth wall casing for reference. While these results are promising, they may not perform the same over a transonic axial compressor hence the need for experimental testing.

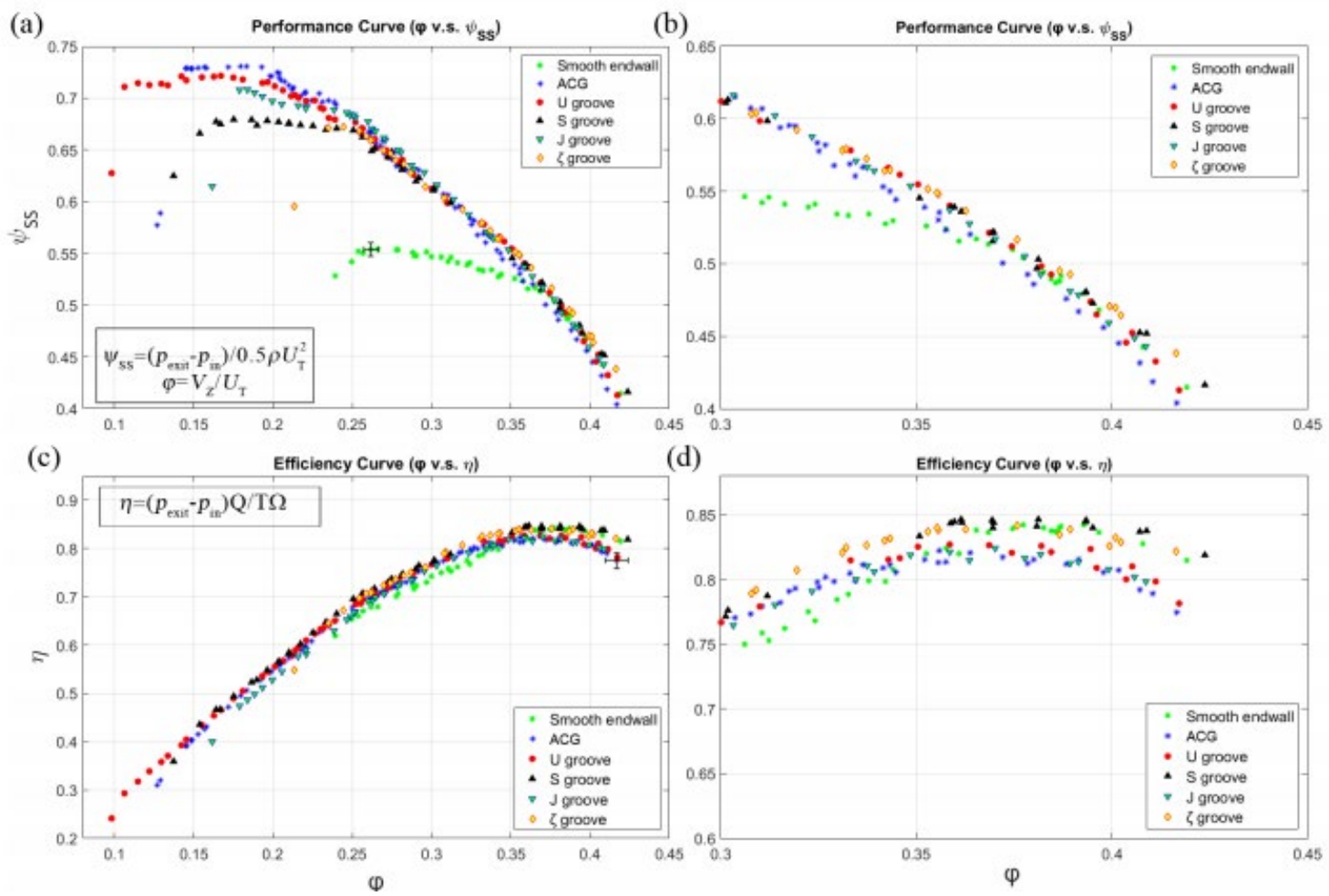

Figure 7. Performance and Efficiency Curves of the Treatments in Figure 6. Source: [4]

Based on the Chen et al. [4] data, the S-grooves were given somewhat of a priority over the U-grooves in producing a casing treated with this geometry. However, there were some key differences between the geometries proposed by Chen et al. [4]. and what was made here. The differences stem from the experimental setups of this transonic study versus the one previous incompressible Chen et al. Also, the geometry of the casing used in this study and the constraints of rotor blade position with respect to the casing edge called for other alterations to their proposed designs. The first change was the number of grooves actually implemented. Instead of the 4 grooves per rotor blade passage tested previously, only 3.8 grooves per passage were able to be fit within the casing inner diameter. Next, the axial position of the inlet and outlet of the grooves were positioned to better reflect the pressure rise across the rotor passage. In 2012, Londono [8] used Kulite probes to measure the pressure in the compressor at different axial locations. Those measurements along with the SolidWorks models for the casing and the rotor blade were used to size the grooves to better suit this experimental setup. Figure 8 shows the pressure contour map made by Londono.

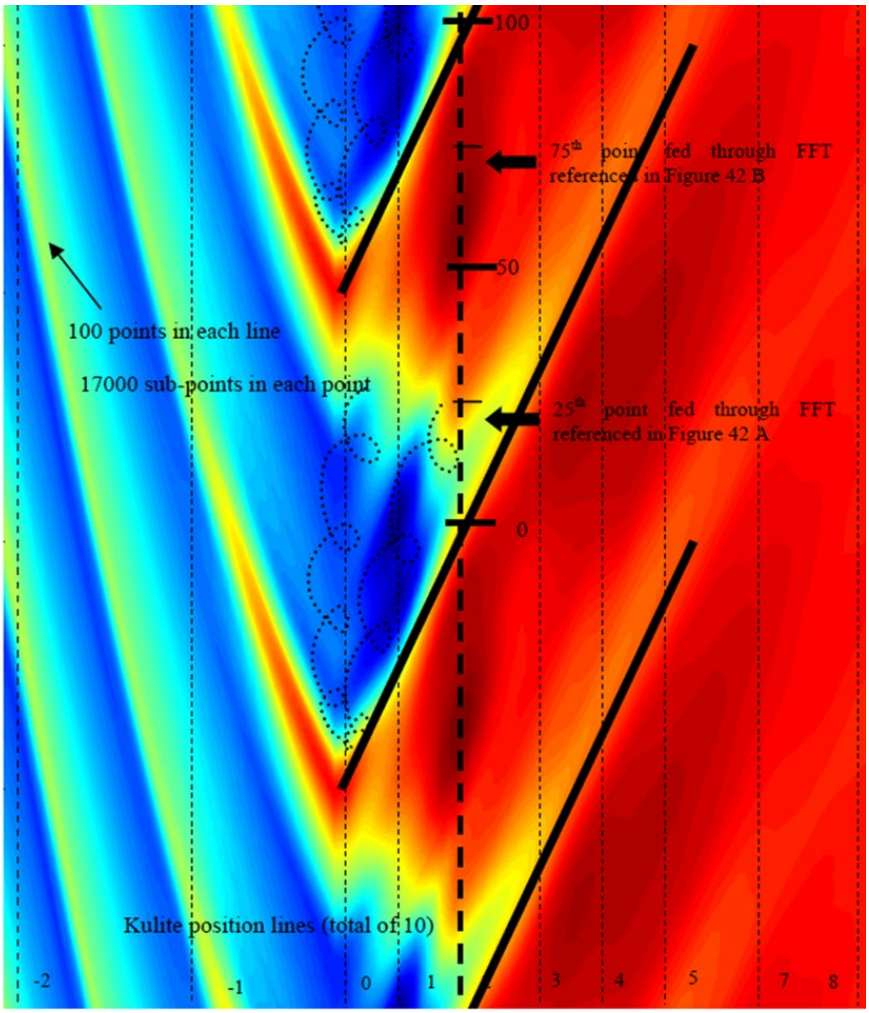

Figure 8. Static Pressure Contour Map. Source: [8]

The pressure map shows that the region of highest pressure in the rotor passage was in the axial location of Kulite probe 2 with the leading edge located at Kulite 0. The lowest pressure region ahead of the rotor blade leading edge was assumed to be halfway between Kulite probes 0 and -1. These locations became the inlet and outlet locations for the grooves, and the width of each groove in the axial direction was based on these locations. Table 1 shows the axial position of the probes measured from the position of a component farther downstream of the compressor casing. The axial length of the groove was calculated to be 22.2mm, (0.874in), by taking the difference of location 2 and average of locations 0 and -1.

Table 1. Kulite Probe Radial and Axial Positions. Source: [8]

Probe Number	Radial Position	Axial Position
Kulite '-2'	-45°	8.5298"
Kulite '-1'	-36°	7.9611"
Kulite '0'	-27°	7.3923"
Kulite '1'	-18°	7.2027"
Kulite '2'	-9°	7.0129"
Kulite '3'	0°	6.8235"
Kulite '4'	9°	6.6337"
Kulite '5'	18°	6.4443"
Kulite '6'	27°	6.2547"
Kulite '7'	36°	5.7997"
Kulite '8'	45°	5.3447"

In order to reduce the flow angle within the groove, the groove was lengthened as far as it could be so until the inlet/outlet of the neighboring grooves overlapped. Furthermore, the inside corners of the inlet and outlet were rounded to increase the amount of casing material, in this case epoxy, between them to preserve structural integrity. The outlet was made to be slightly narrower than the inlet to provoke a velocity increase through the groove. These modifications are shown in Figure 9.

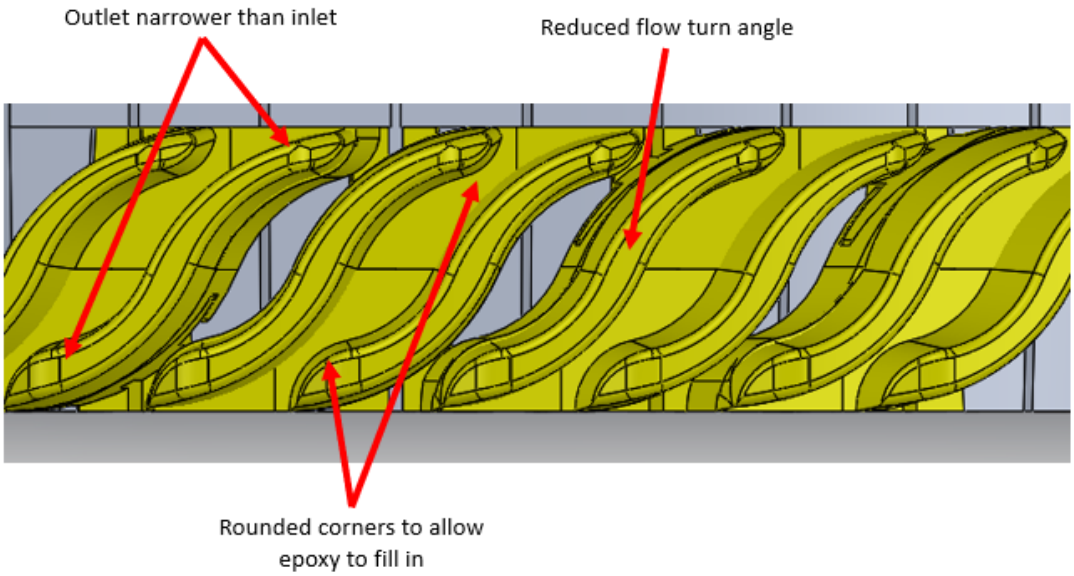

Figure 9. Modifications to the Proposed S-Grooves

The following section will discuss the final designs for the surface casing treatment molds and accompanying parts that were used to implement this treatment.

B. FINAL DESIGNS

The compressor casing that the treatments would be applied to in this study is on the transonic compressor test rig, (TCR), of the Naval Postgraduate School, (NPS). The outer components of the casing are made of aluminum, and the inner wall closest to the rotor blades is made of epoxy. The epoxy layer is there to provide a more abradable surface in the event the rotor blades scrape the casing wall during operation. West Systems 105 Epoxy Resin and West Systems 410 Microlite Filler were used to form the epoxy layer. In order to create the most structurally sound epoxy layer, it would need to be one solid piece poured at one time. To set the epoxy in the circular shape of the casing, it has to be poured into the casing while turning on a lathe. An aluminum ring on either side of the casing inner wall dams the epoxy during this process and remains a component of the final product. Figure 10 displays a cross section of the casing inner wall and Figure 11 illustrates the formation of the epoxy endwall.

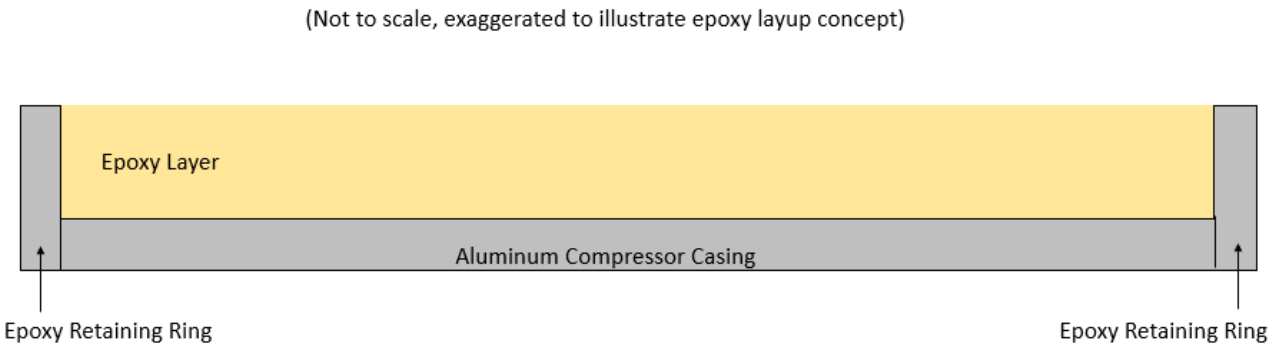

Figure 10. Compressor Casing Epoxy Layer Cross Section Diagram

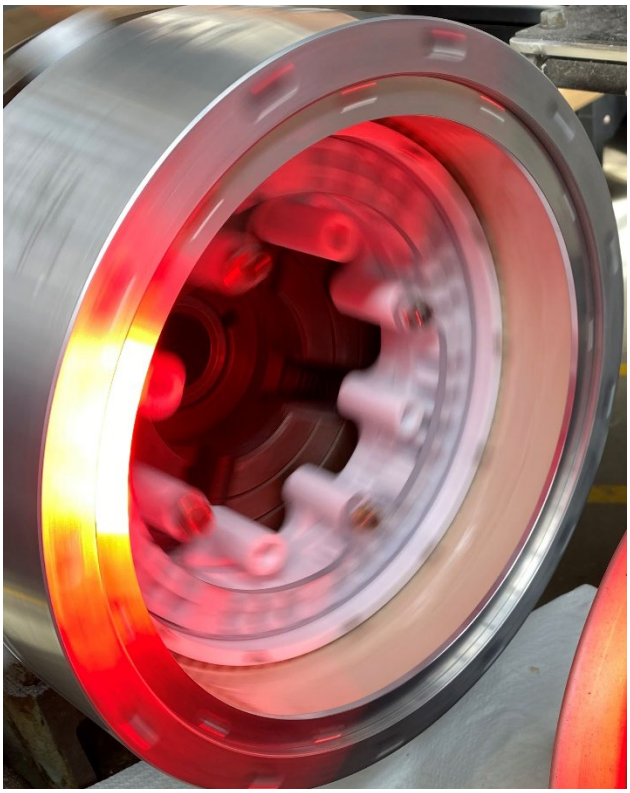

Figure 11. Epoxy Layer Layup on Lathe

The inner surface of the aluminum casing that meets the epoxy is grooved to provide a stronger grip for the epoxy after curing. However, the grooves were machined out in this study leaving a smooth inner diameter for the aluminum casing. This was done

to make more space available for treatments. The design process is based on the idea that complex geometries would need to be cast into the epoxy layer while on the lathe, with molds made by additive manufacturing. Designing parts was done initially with concept sketches with final geometries modeled using the program SolidWorks. Once the part designs were modeled and there were no obvious errors in their concepts, they were prepared for 3D printing using the Cura software by Ultimaker. These test parts were then printed using an Ultimaker 3 Extended printer with polylactic acid, (PLA), and polyvinyl alcohol, (PVA). The final versions were printed in polycarbonate by a Stratasys printer.

If molds were to be used to cast the grooves into the epoxy layer, an attachment piece would be needed to hold all of the molds in place while on the lathe for epoxy layup. A large disk was designed to attach to the casing and secure the molds locations. Figure 12 and Figure 13 show the SolidWorks model for this part.

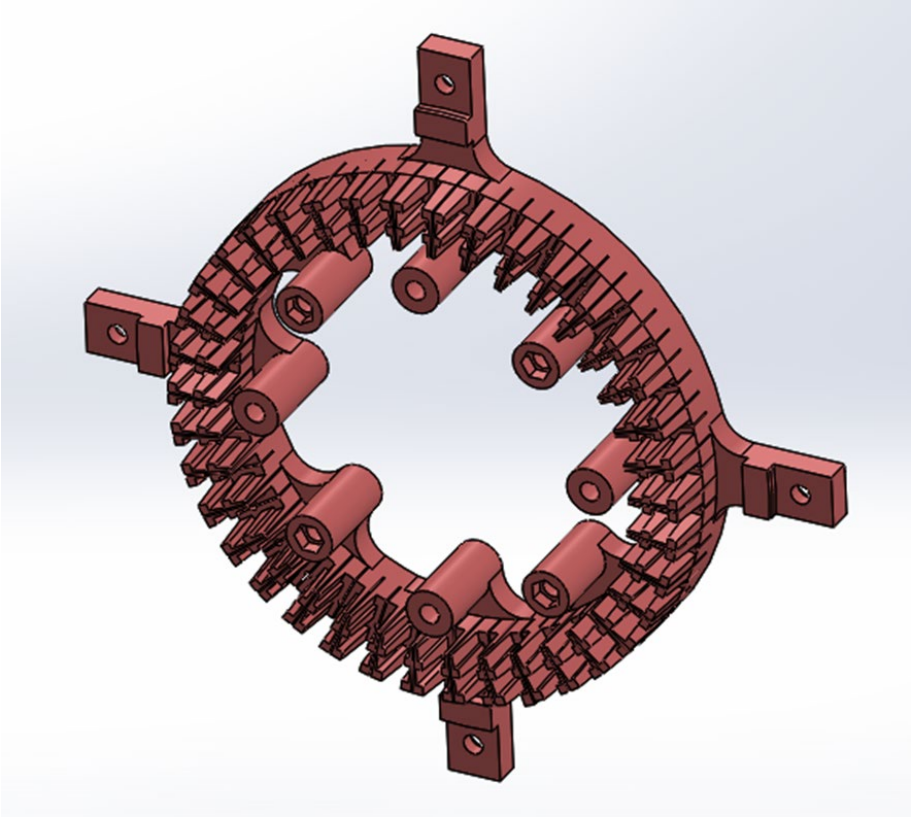

Figure 12. Main Disk SolidWorks Model

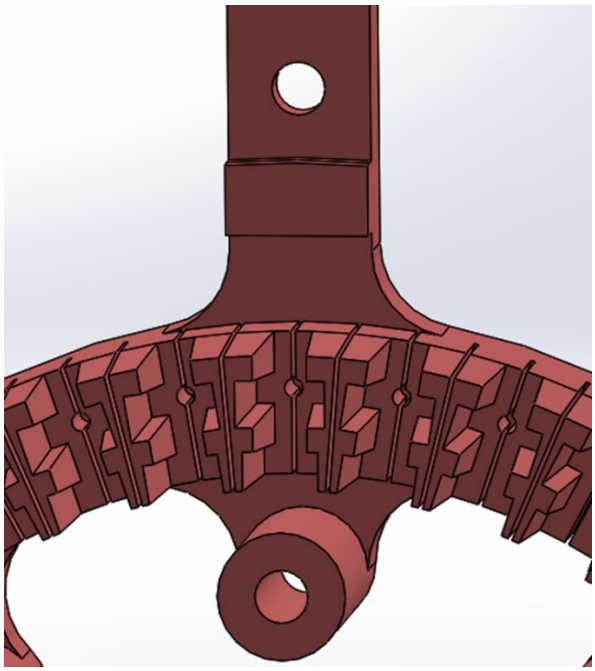

Figure 13. Main Disk SolidWorks Model Zoomed In

The main disk consists of four arms that extend to the outer edge of the casing where it is bolted in place. On the inside face of each arm is a block that aids in keeping the disk position steady while on the lathe. The disk protrudes into the casing center where 38 slots are aligned circumferentially to hold the molds. In between and down the center of each mold location is a smaller slot that allows for elastic deformation of the main disk when the molds are inserted. These slots were an addition to the design that was made in response to difficulties removing molds from test prints. In the center of each mold location is a small hole that extends to a flat surface from which the molds utilize a captured nut and bolt to push off the main disk after the epoxy is cured. The innermost edge of the main disk harbors eight tubular passages that either serve to attach a retaining disk, (discussed later), or capture a nut that can be used with jacking screws to aid in removing the disk after the epoxy has cured.

Of the groove geometries examined, the S-shaped and U-shaped grooves were the only ones modeled in SolidWorks, and the S-Shaped groove was the only one printed for testing. As evident from the slots on the main disk, the molds are held in place by T-slots on the mold base. Both the S and U-shaped grooves utilize the same base with some minor

exceptions which are discussed later. Figure 14 shows the S-shaped groove mold for visualization. Note that each mold, shown in yellow, has two grooves attached to it so that 3.8 grooves per rotor blade could be achieved.

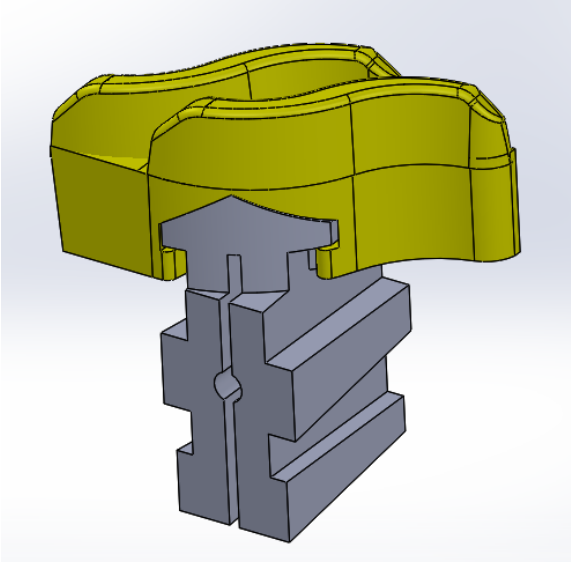

Figure 14. S-Shaped Groove Molds

The most important part of each mold is the top because that is the only part that will be cast into the casing wall. Figure 15 shows the tops of the molds when placed in the main disk.

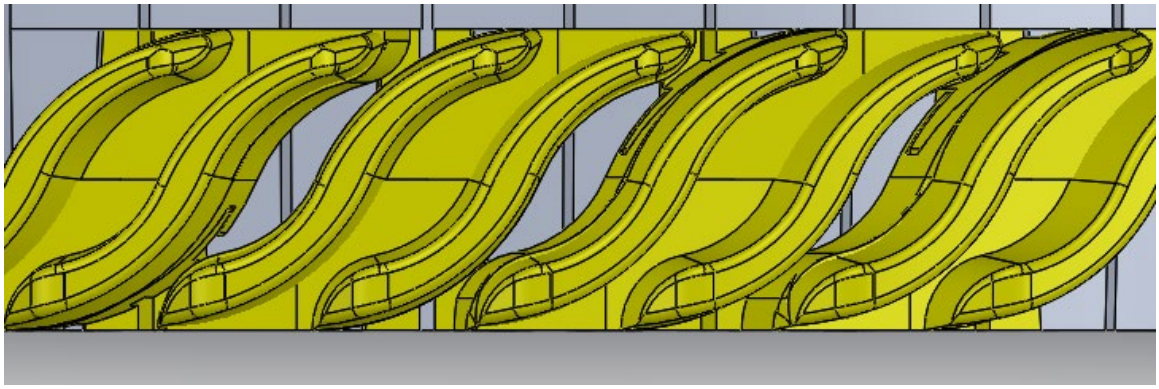

Figure 15. S-Shaped Grooves in Line on Main Disk

The circumferential length of each groove was 28.448mm, (1.12in). The SolidWorks sketch of the mold before 3D extrusion can be seen in Figure 16.

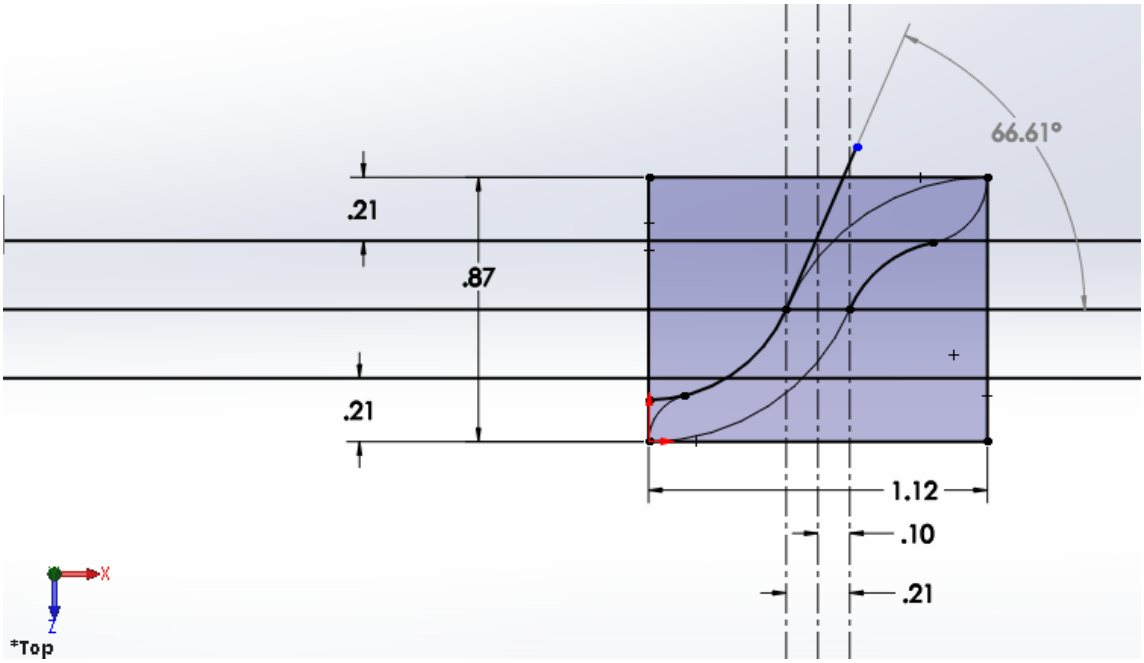

Figure 16. Two-Dimensional Sketch of the S-Shaped Groove (Dimensions in Inches)

The SolidWorks cavity feature was used to show how the molds would cast the grooves into the epoxy layer before each test print. This along with the relative position of the rotor blades can be seen in Figure 17 and Figure 18.

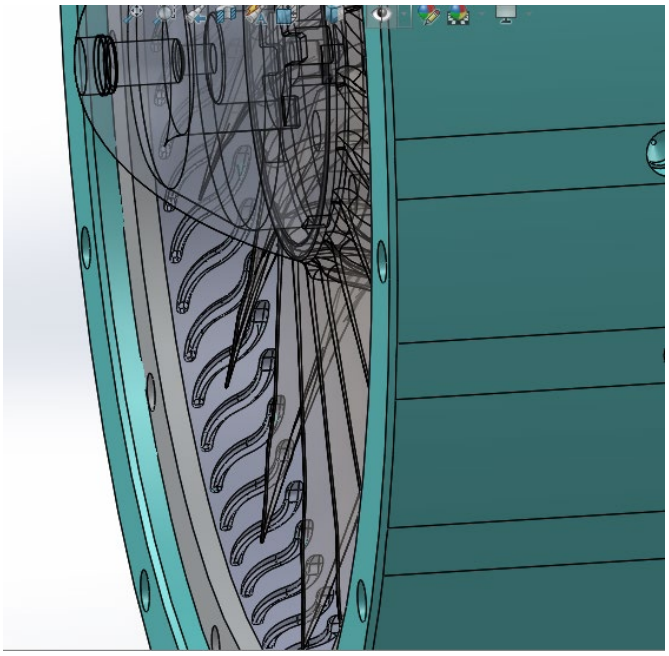

Figure 17. SolidWorks Representation of S-Grooves Cast into Epoxy Layer

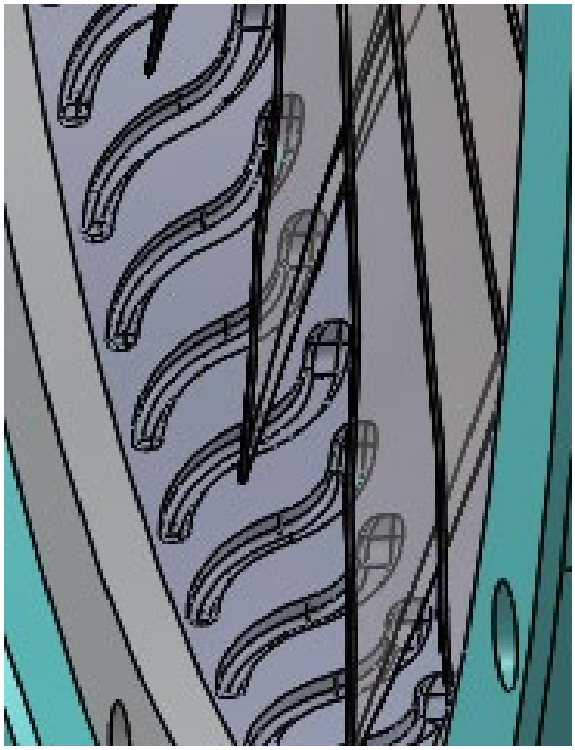

Figure 18. Zoomed In View of S-Grooves Cast Into Epoxy Layer

The upper end of each groove in Figure 18Figure 17 represents the inlet of the groove, and the bottom is the outlet. In theory, the high-pressure air at the inlet would travel through the groove to the low pressure region at the outlet and then back through the rotor passage, reducing radial flow velocity, and delaying the onset of stall.

Once the epoxy cured and the casing could be removed from the lathe, the main disk and 38 molds would need to be removed. Appendix B describes a short test involving epoxy that led to the decision to print the mold tops in water-soluble PVA. To remove the molds and main disk, the mold tops would only need to be dissolved, (or mold bases pulled off), and all parts could be removed at one time. The mold tops were designed to attach to the polycarbonate bottoms using the geometry shown in Figure 19 through Figure 22. It relied on friction to prevent movement and the elasticity of the PVA tops to snap into place on the two notches on the side of the base.

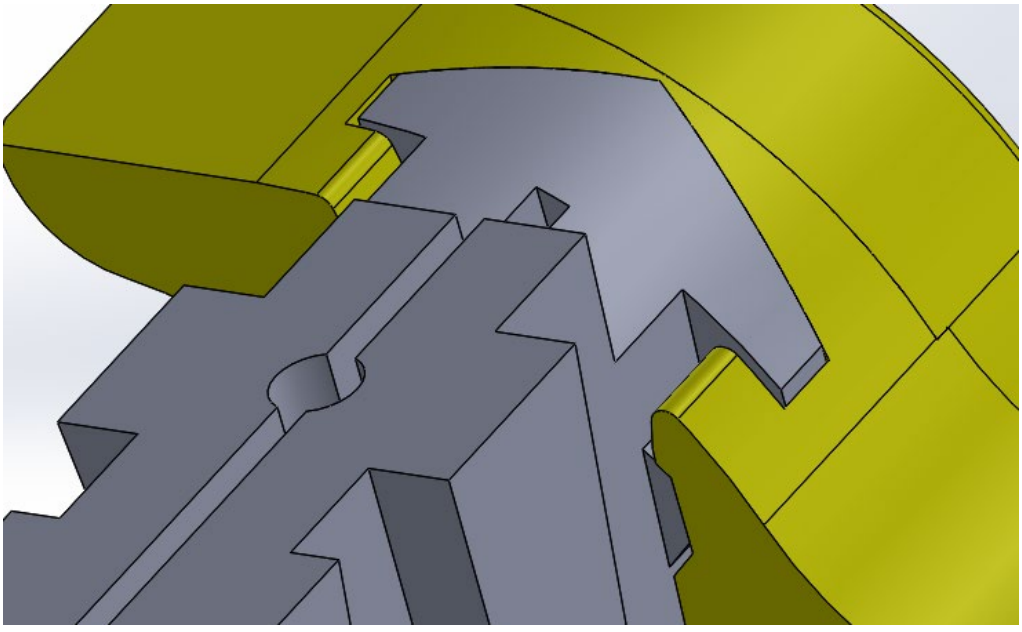

Figure 19. S-Mold Base and Top Connection

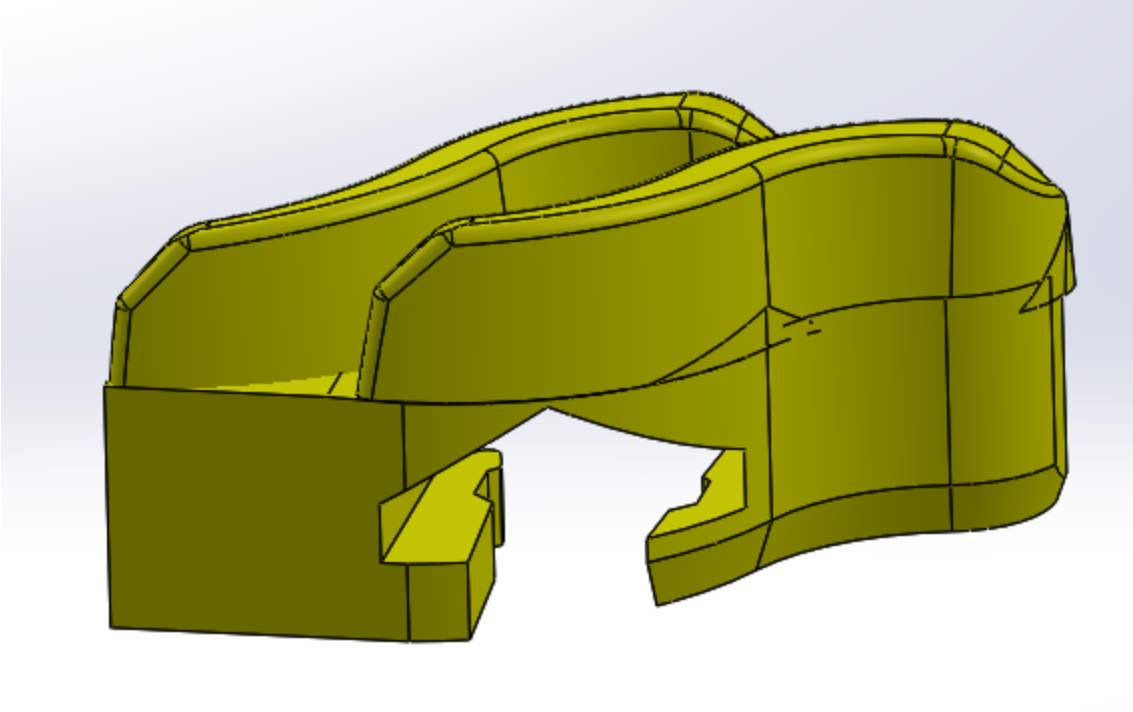

Figure 20. PVA Mold Top Front View

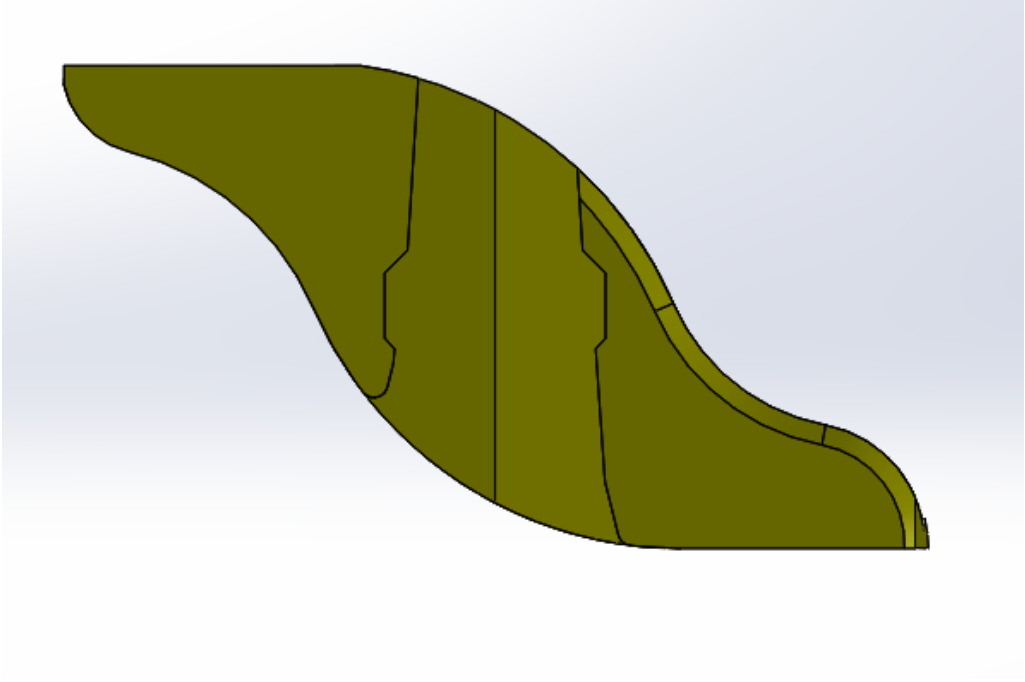

Figure 21. PVA Mold Top Bottom View

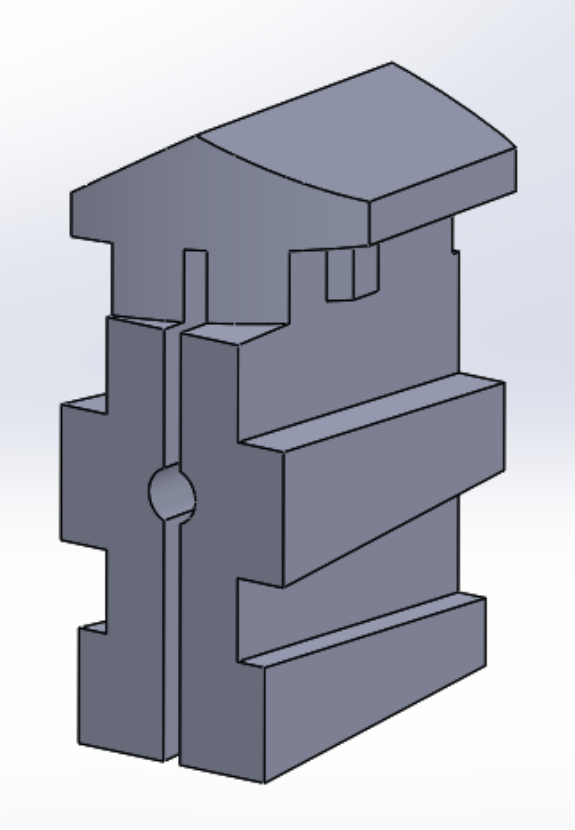

Figure 22. Polycarbonate Mold Base

In the figures the PVA soluble material that will form the grooves is shown in yellow while the mold base is shown in gray. The PVA tops were rounded to match the curvature of the casing inner face. By making the molds tangent to the casing, it was assumed that very little, if any, epoxy would be able to fill in the small gap between the molds and casing. This and the position of the molds relative to the casing and each other can be seen in Figure 23.

Figure 23. Molds in Place on Casing Zoomed In

Removing the mold bases from the main disk was done using a captured nut. By turning a bolt through the nut and all the way to the flat surface on the main disk, the nut was able to push the mold bases out of the main disk. This concept is shown in Figure 24.

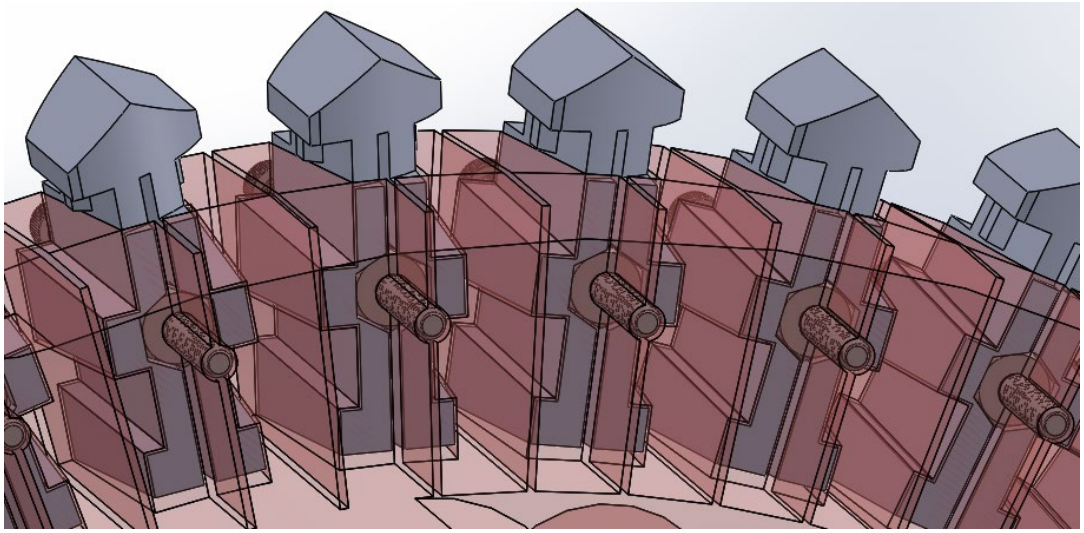

Figure 24. Captured Nut System

In order to hold the molds tight to the main disk while on the lathe, a retaining disk was designed to prevent movement in the axial direction. Because the disk is relatively simple in design, it was made out of clear polycarbonate and cut with a water jet. The retaining disk model in SolidWorks can be seen in Figure 25 .

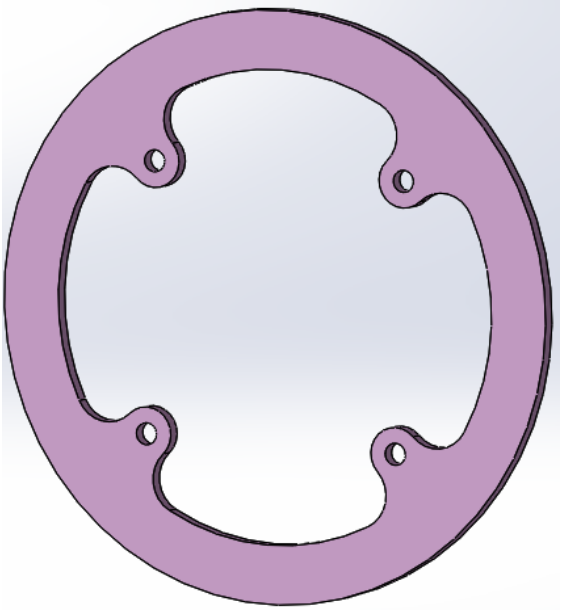

Figure 25. Retaining Disk SolidWorks Model

The retaining disk is mounted to the main disk with four socket head screws. The next section will show the implementation process and how each of the described parts interact. To show all of the parts and hardware involved in the surface casing treatment process, Figure 26 shows an exploded view of the SolidWorks models.

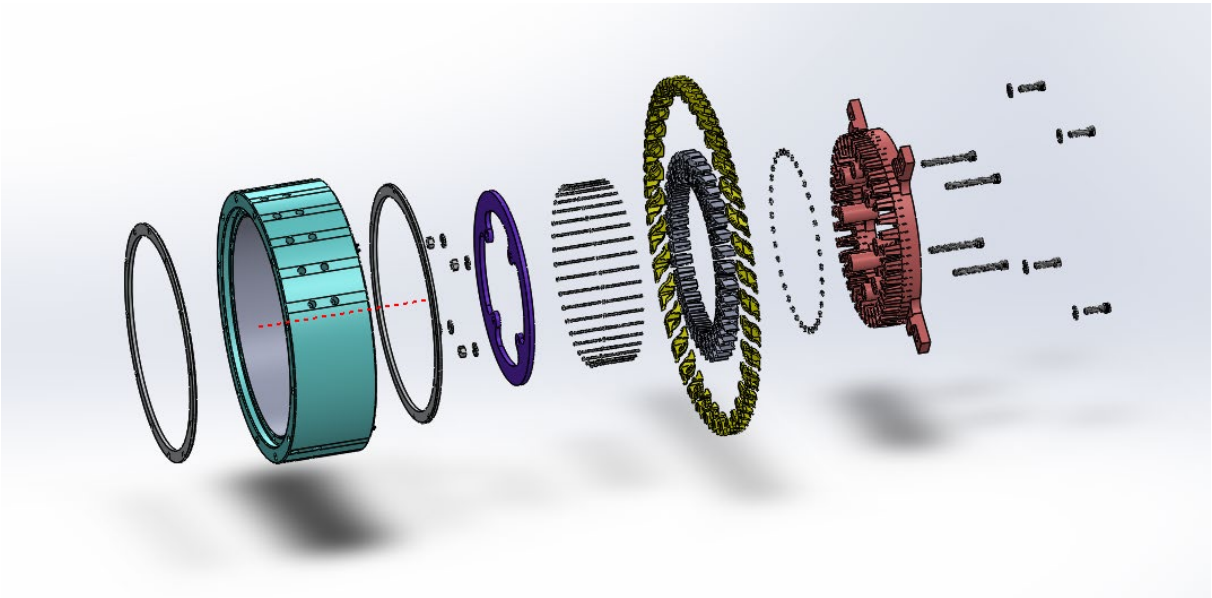

Figure 26. Exploded View of Surface Casing Treatment Process

C. SURFACE CASING TREATMENT MANUFACTURING PROCESS

The first step in preparing the mold and casing for treatment is to remove the retaining ring from the front edge of the casing. It must be placed on the main disk as shown in Figure 27 before the molds are inserted. Neglecting this step will prevent the main disk from fitting on the casing.

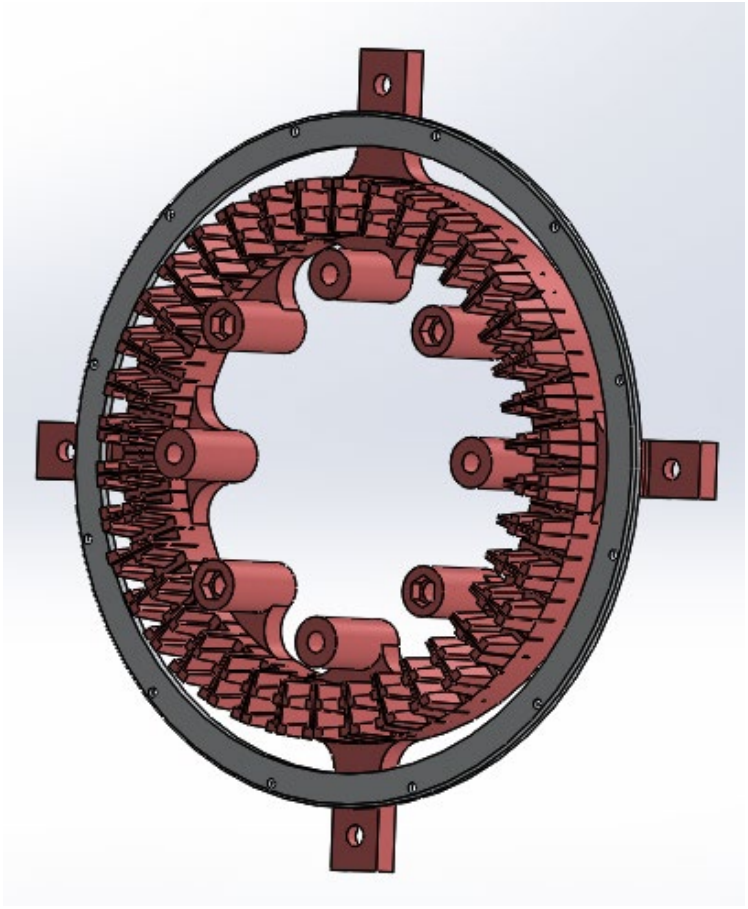

Figure 27. Retaining Ring on Main Disk

Next, the tops of each mold must be attached to a base. This is done in a sliding motion until the PVA top clicks into place. Then, a hexagonal nut can be placed behind of each mold as shown in Figure 28. Once all of the molds have a captured nut, they may be inserted into the main disk one at a time as shown in Figure 29. Note, the first mold inserted will need to be raised in order to insert the final mold due to overlapping inlets and outlets.

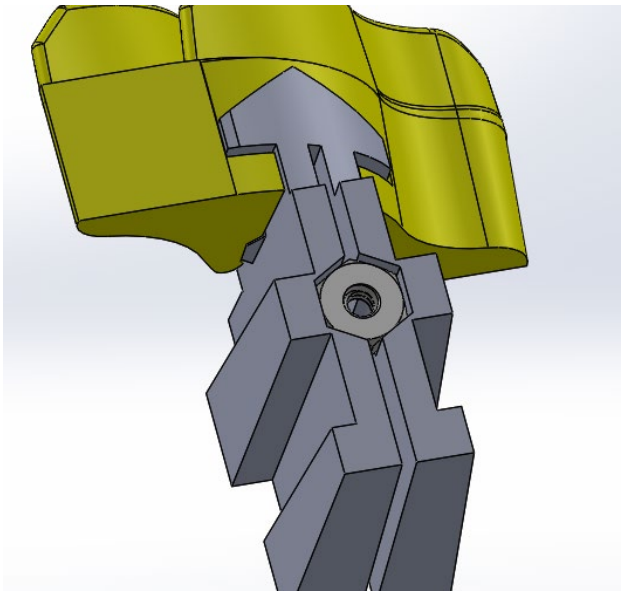

Figure 28. Axial Captured Nut Placement

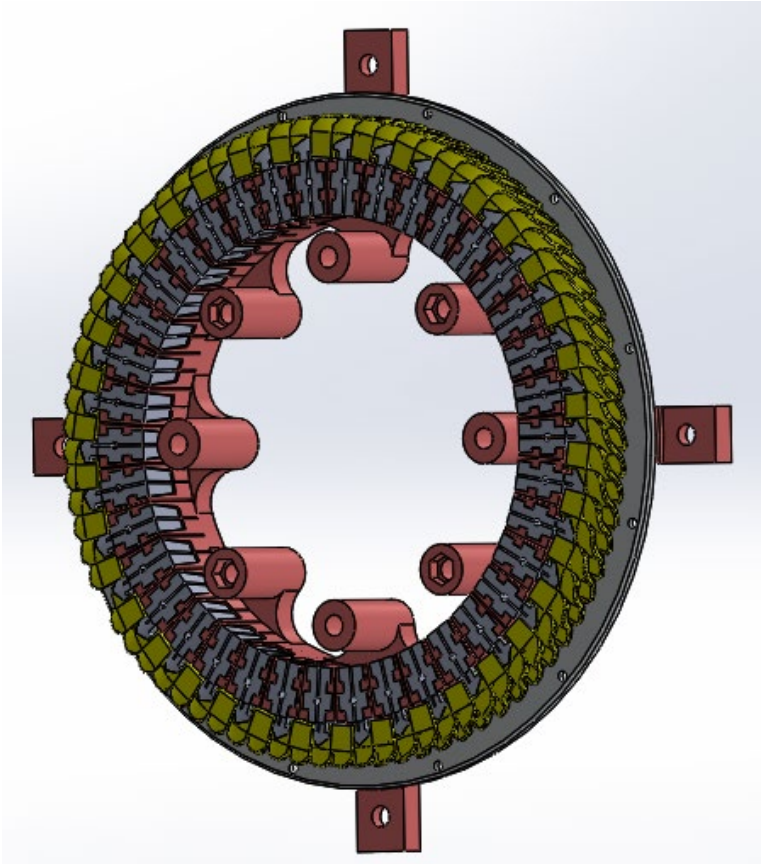

Figure 29. Molds in Place on Main Disk with Retaining Ring

The next step is to use the hardware shown in Figure 30 and Figure 31 to attach the clear retaining disk to the main disk, (it is shown in pink in Figure 30 and Figure 31).

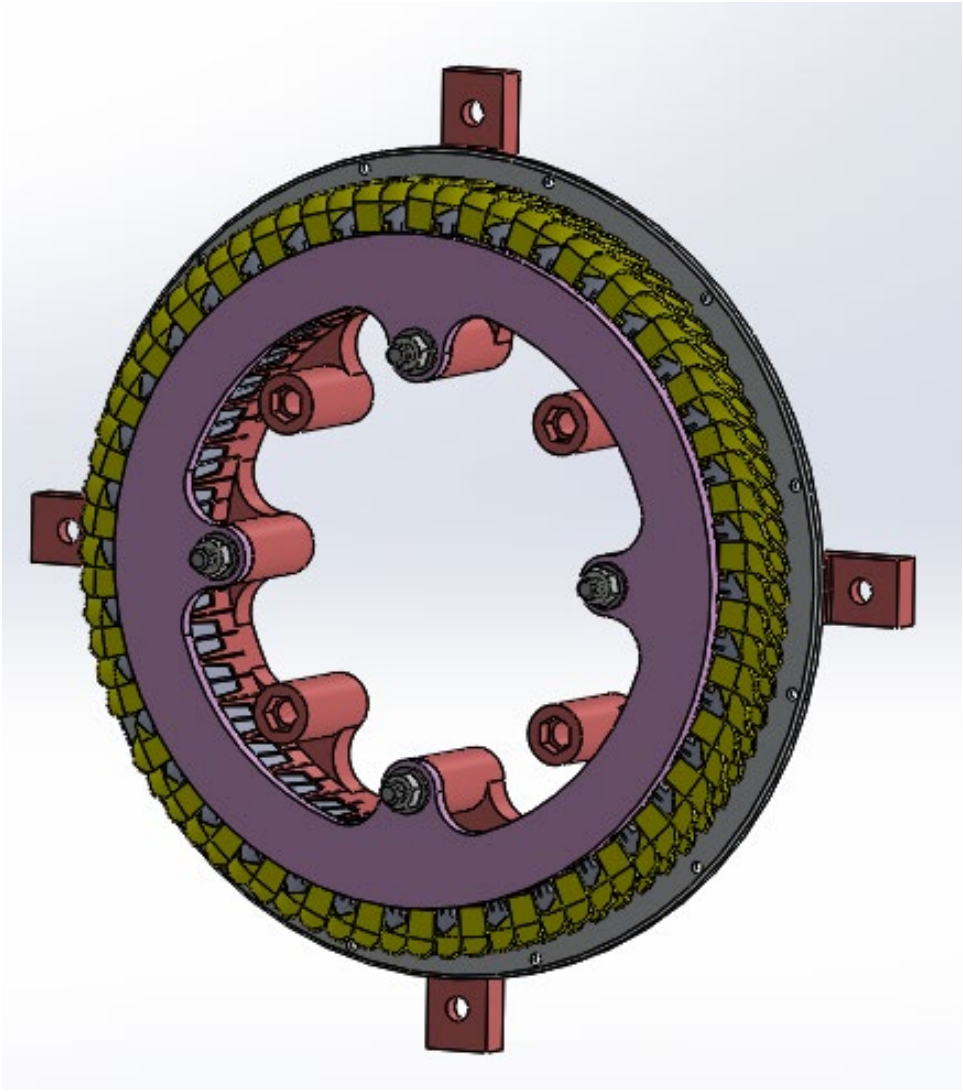

Figure 30. Retaining Disk Attachment Front

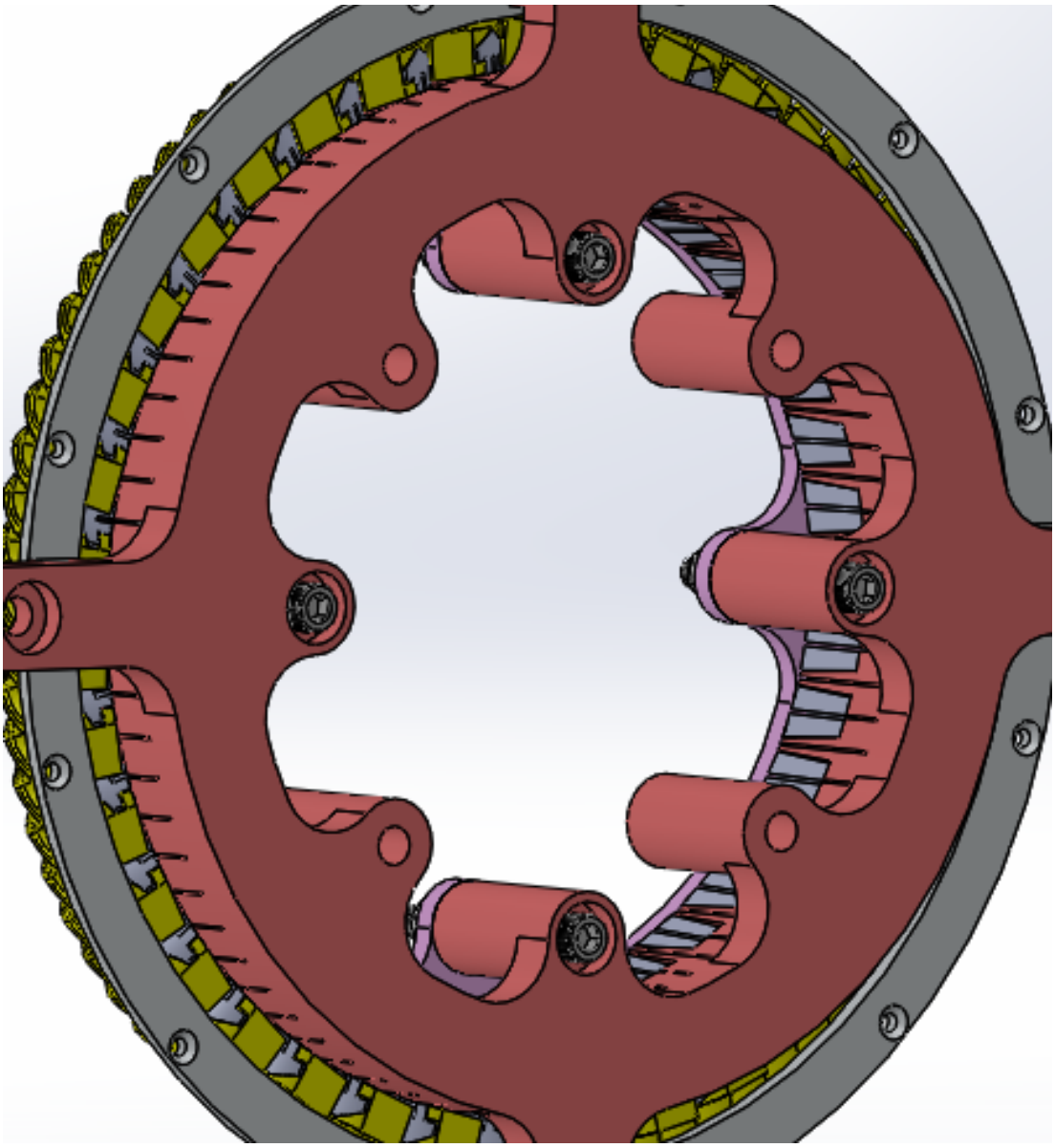

Figure 31. Retaining Disk Attachment Rear

After that is done, the entire system is ready to be attached to the compressor casing. Threaded inserts are already in place on the casing, which the four arms of the main disk connect to using bolts as shown in Figure 32.

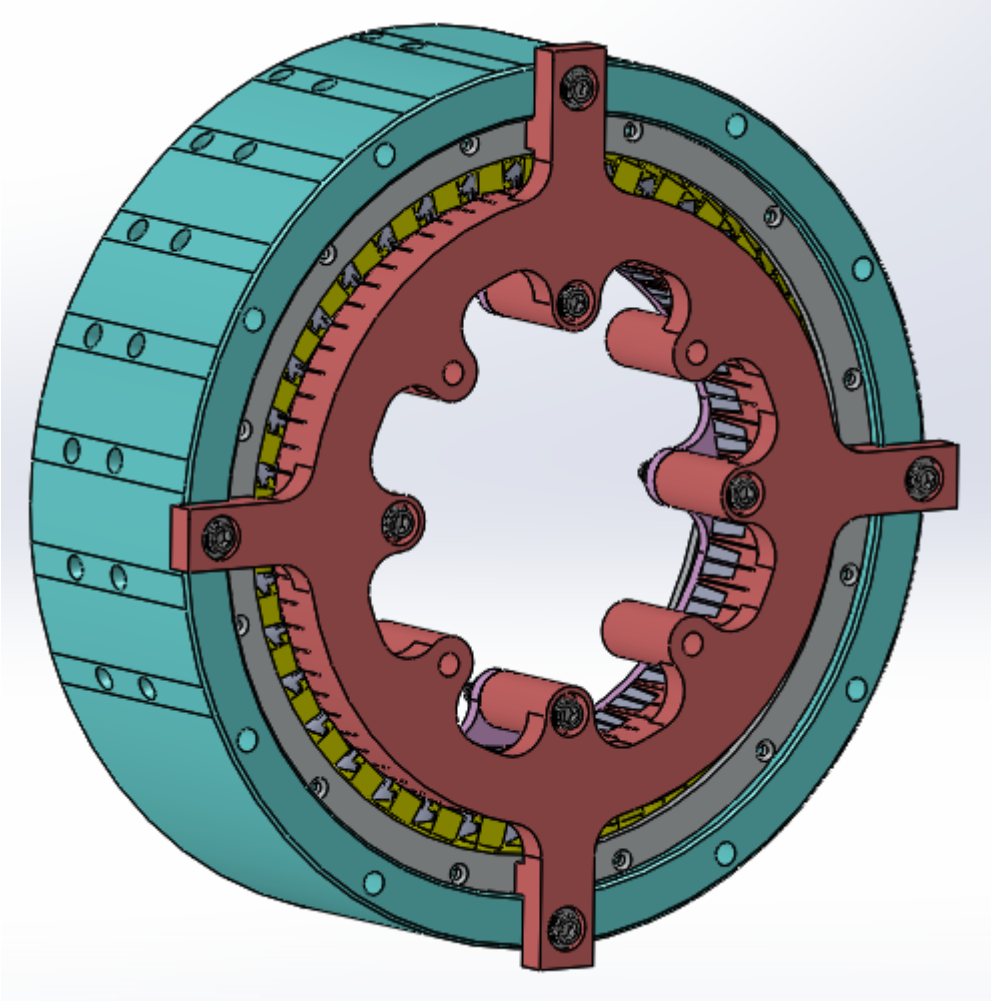

Figure 32. Surface Treatment Assembly Attached to Compressor Casing

Once the parts are bolted ono the casing, the casing may be put on the lathe as shown in Figure 33 and Figure 34. It is important to center the casing on the center of the chuck as closely as possible to ensure even rotation.

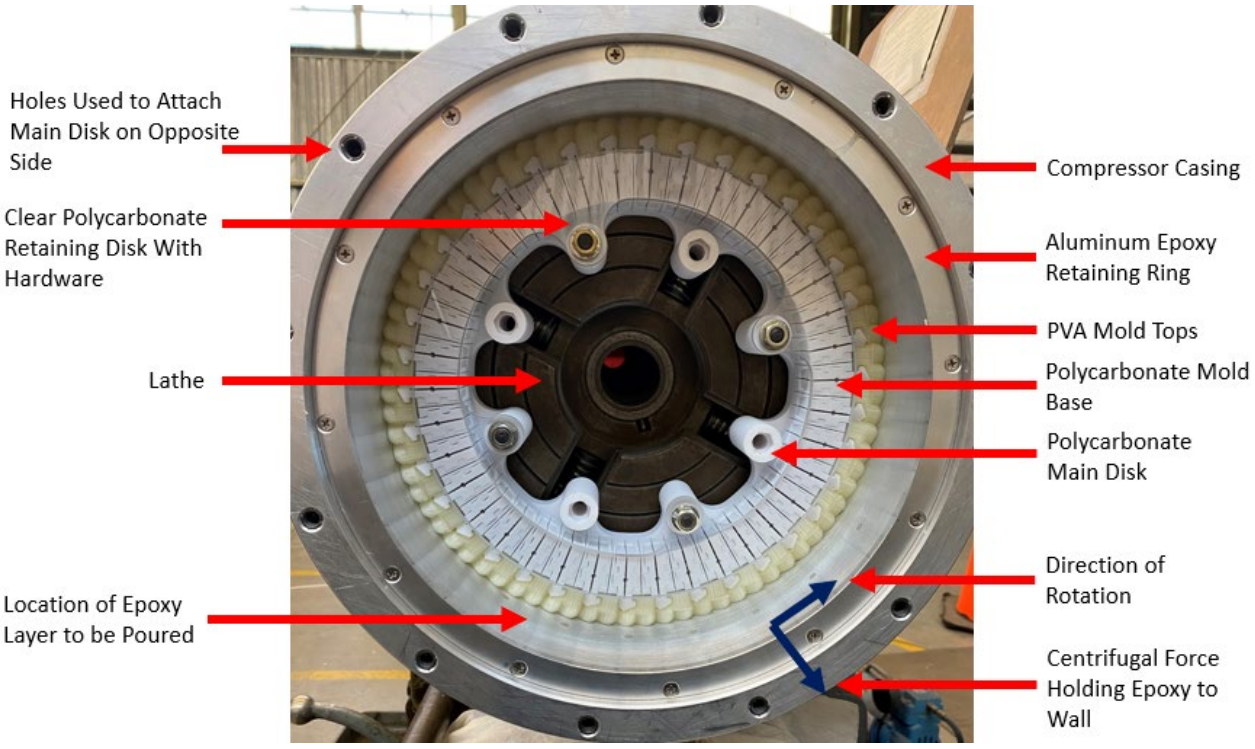

Figure 33. Surface Casing Treatment Assembly on Lathe Front View

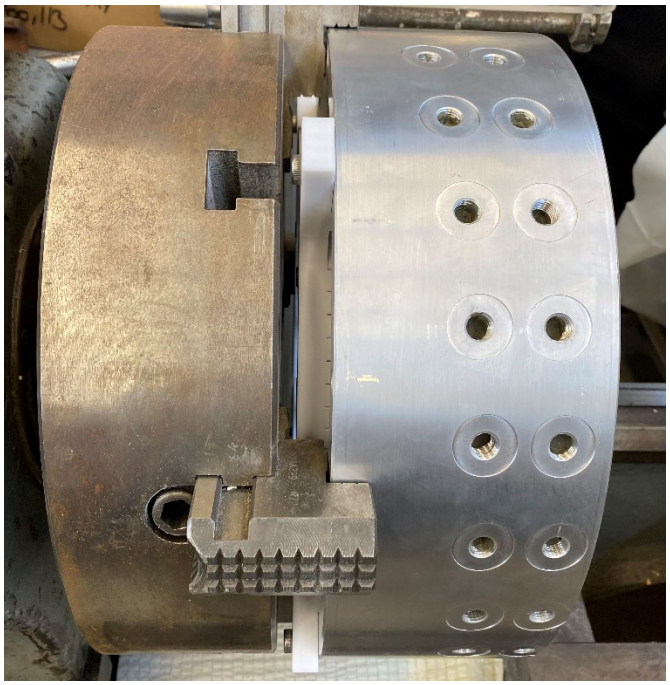

Figure 34. Casing on Lathe Side View

From here, the lathe may be turned on and the epoxy slowly poured. It is recommended that at least 24 hours pass before stopping the lathe. Figure 35 shows the casing turning during the epoxy layup. Note that a heat lamp was placed nearby to aid in the curing process.

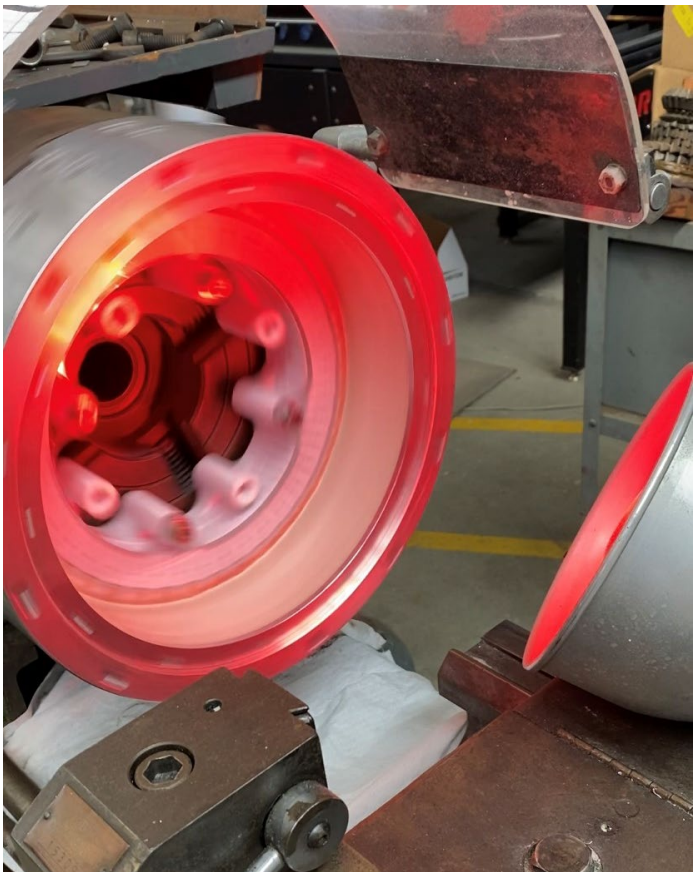

Figure 35. Surface Casing Treatment Epoxy Layup

Once removed from the lathe, the four bolts on the main disk arms, and the retaining disk were removed. Removing the main disk was done using the captured nut described in Figure 24. A bolt was inserted into each mold and was turned a very slight amount until the main disk was removed and all that was left was the molds. Figure 36 shows the bolts in place in each mold for the main disk removal.

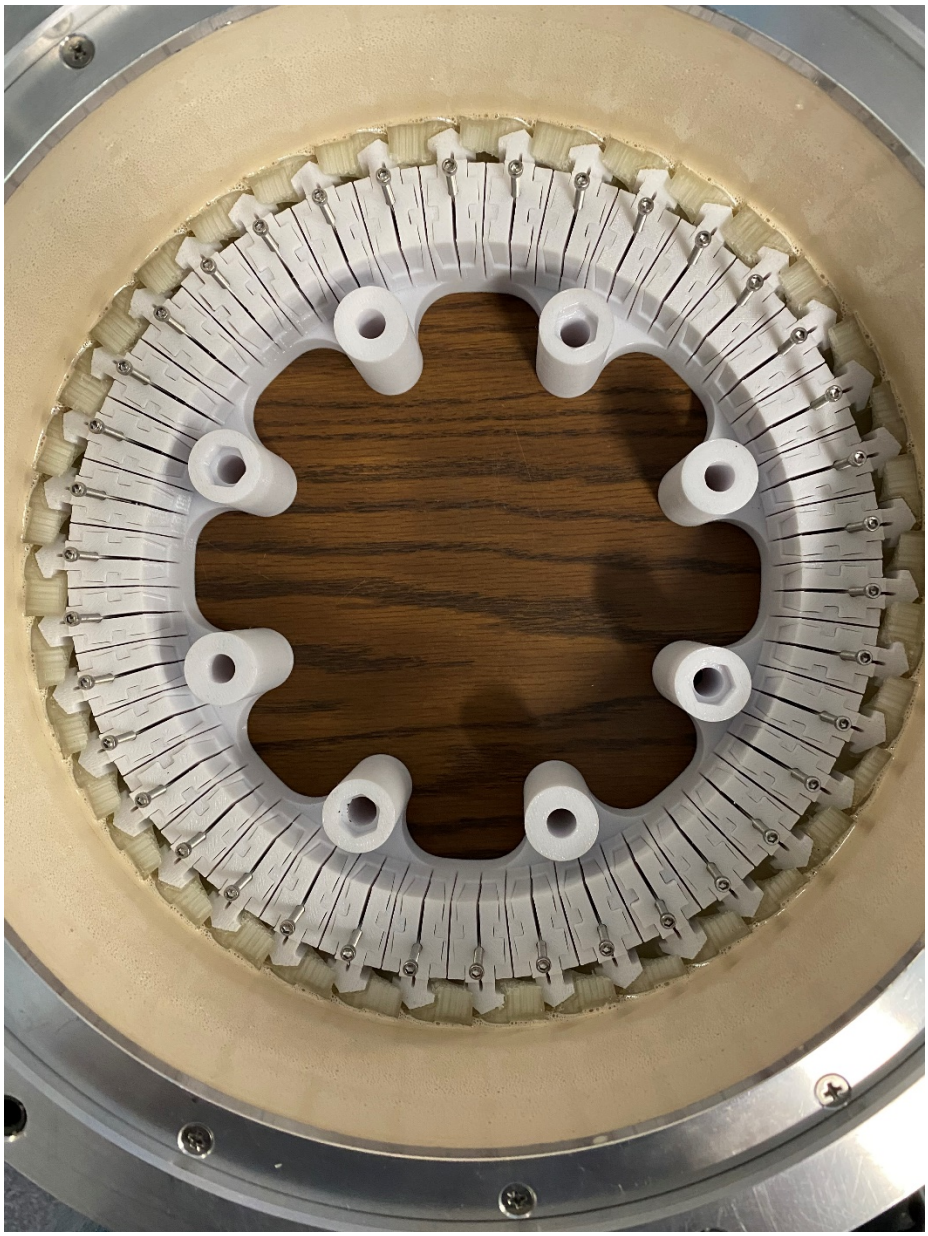

Figure 36. Main Disk Removal

Notice the bolts in each mold in the figure. Once the main disk and removed, the mold bases followed. The results of this treatment are discussed later.

III. DESIGN OF THE INTERNAL PASSAGE CASING TREATMENT

A. BACKGROUND

The second part of this work deals with the manufacture of treatments in the form of internal passages. A report from Hathaway [6,7] outlines his method of recirculating flow via decoupled and coupled bleed and injection ports downstream and upstream of the rotor, respectively. The recirculation paths were tubes that extruded from the compressor bleed port and looped back into the injection port. Figure 37 shows his experimental setup and Figure 38 shows the injection port locations spread around the circumference of the casing.

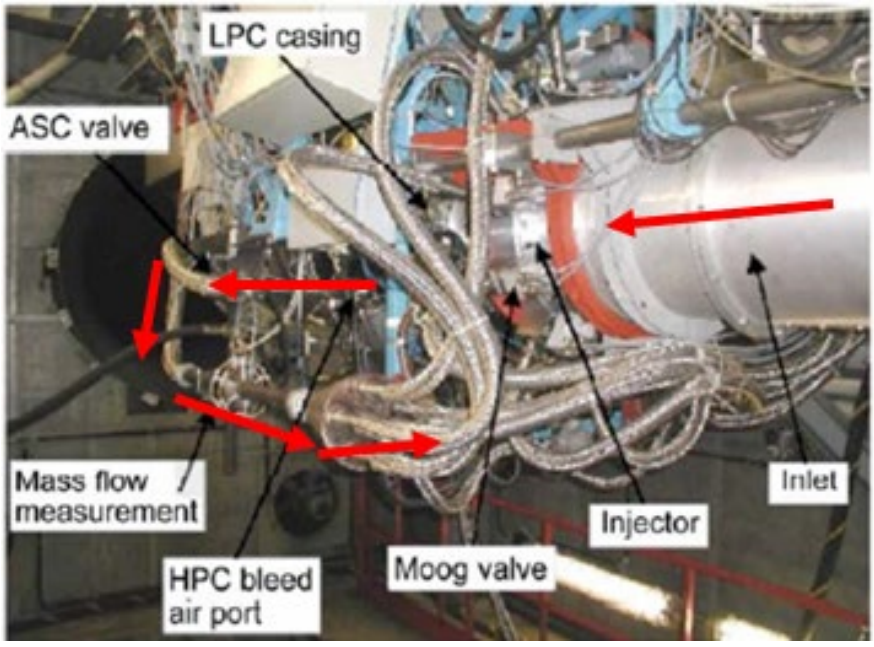

Figure 37. Flow Recirculation System Created by Hathaway. Adapted from [7]

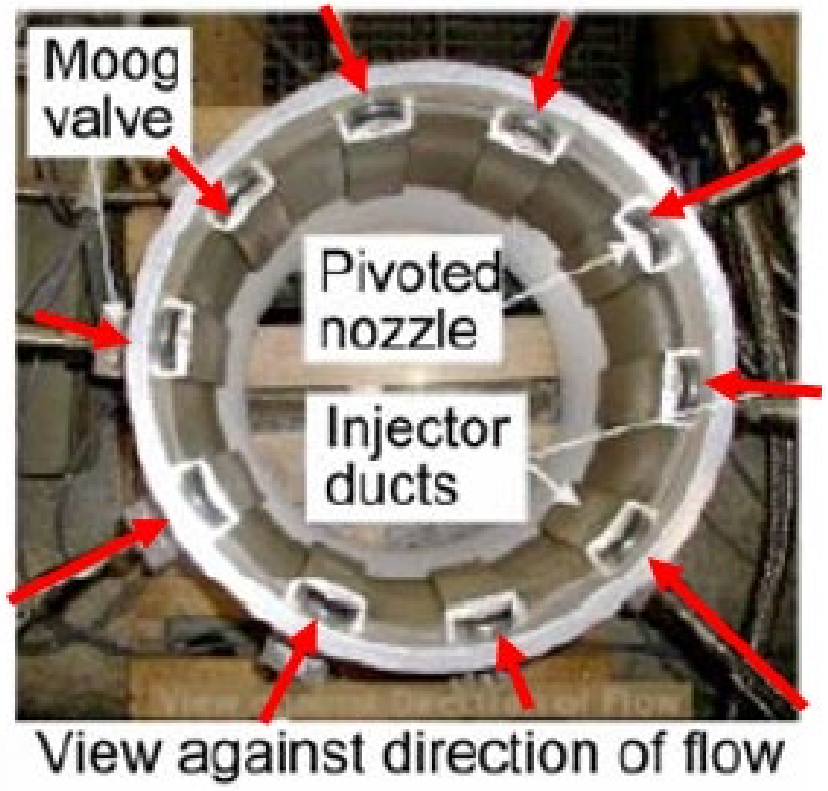

Figure 38. Injection Ports of Recirculated Flow. Adapted from [7]

The red arrows indicate the movement of air starting at the inlet and traveling though the casing recirculation treatment. The Moog valve shown in Figure 38 is a servo valve used to open and close the injection ports. The treatment achieved a 225% increase in stall margin while only incurring a 5% loss in adiabatic efficiency. Figure 39 displays his results. An important feature of Hathaway's study was the inclusion of inlet distortion that would better model a practical scenario as opposed to only examining ideal inlet conditions.

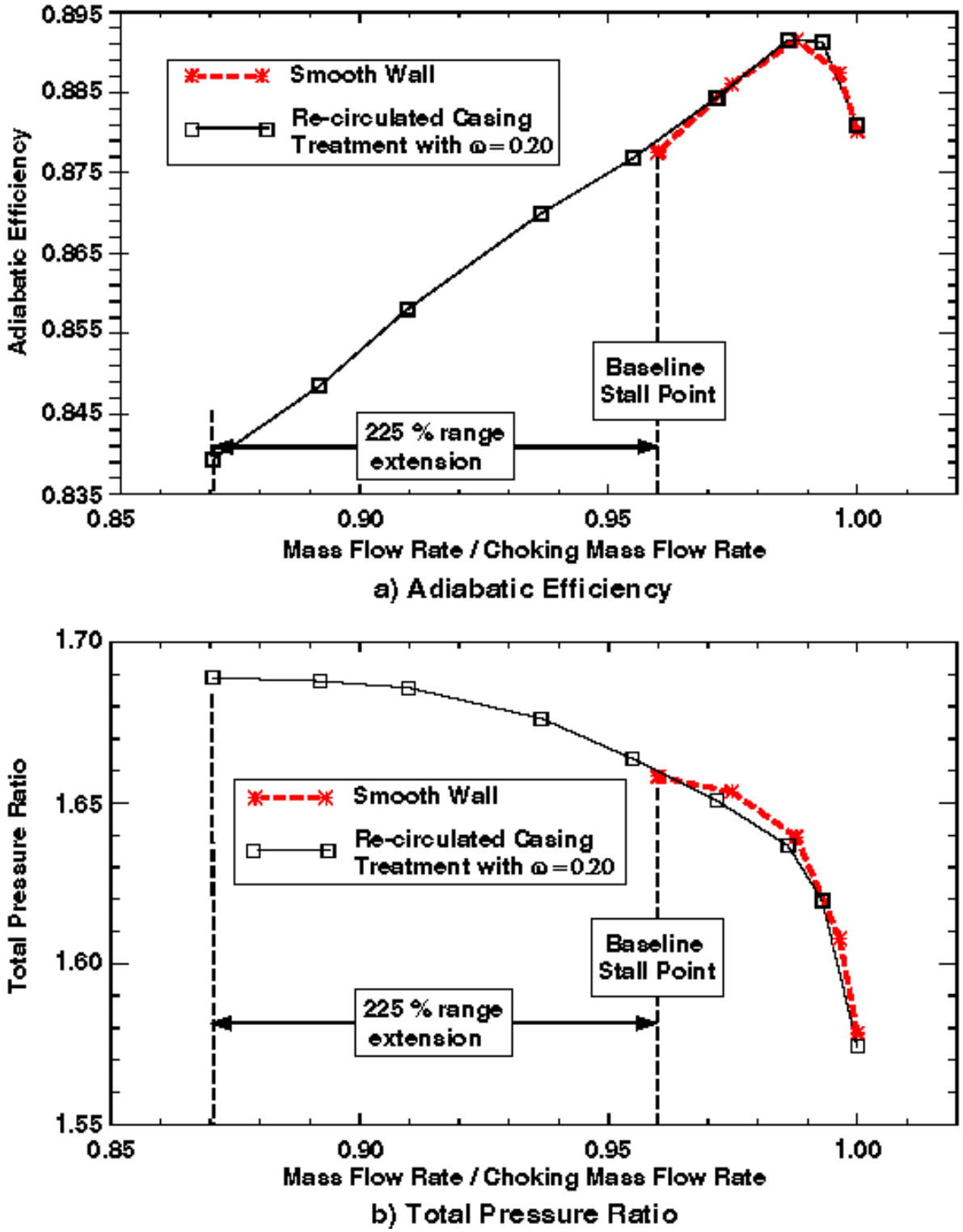

Figure 39. Recirculated Treatment Applied with Inlet Distortion.
Source: [7]

Due to the size constraints of the TCR compressor casing, this study aims to achieve similar results without having the passages exit the thin layer of epoxy coating the compressor casing.

B. SIZING THE INTERNAL PASSAGES

The main concept for implementing internal passages in the epoxy layer of the casing is very similar to that of the surface treatments. The same main disk would hold passage molds while on a lathe. The passages were made out of PVA support material because it is water-soluble. This way, the entire casing could be submerged in water or sprayed with a jet of water until the molds dissolved, leaving behind tunnel-like structures in the epoxy. Because the epoxy layer is thin, the casing diameter needed to be increased to allow for larger passages. The casing was put on a lathe and the diameter was increased so that 0.00127m, (0.05in), remained between the casing inner surface and the screw holes for the epoxy retaining rings. While making sure that 0.00254m, (0.1in), of epoxy remained between the passages, the cross section of the rectangular passage was set to be 0.0024m, (0.095in), by 0.0027m, (0.105in). This made for a cross sectional area of 6.435E-6m^2, (0.009975in^2). This was the largest possible size that would not infringe on the structural integrity of the casing or epoxy layer. Being able to print a passage that is hollow was one of the needs for the largest passage possible, as was more mass flow per passage. Figure 40 shows the SolidWorks model of the passage mold.

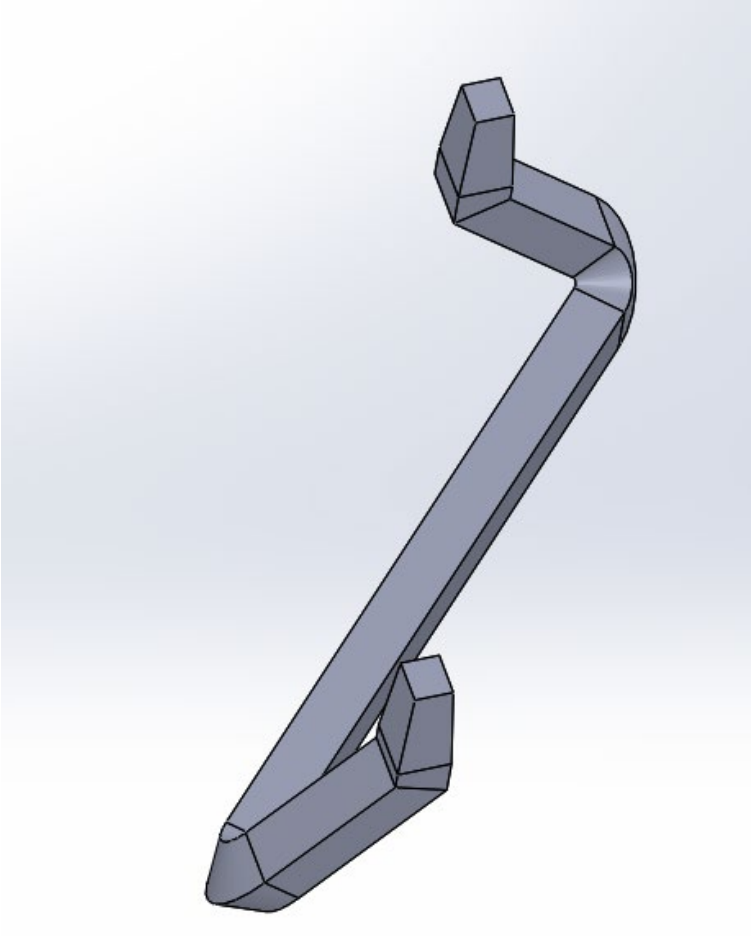

Figure 40. Internal Passage Molds from Multiple Angles

The length of the passage from bleed to injection was determined by axial length of the rotor blade passage. It is suspected that the injection port location with respect to the rotor blade leading edge has a greater influence on the effectiveness of the treatment than the bleed location with respect to the blade trailing edge. Therefore, the passage was made long enough to be able to shift the casing in the axial direction without bringing the bleed port too far forward of the trailing edge. The injection port with respect to the epoxy retaining ring is as close as it could be without raising concern about the epoxy thickness between the retaining ring and the port. The bleed port location was also constrained by a shrouded stator blade row following the rotor. The inlet and outlet both bend at 45º in the vertical and horizontal planes in order to better bleed/inject flow, respectively. Because the passages were small in size, friction within the passage could not be ignored. However,

because the flow would be in it for a short time, heat transfer was assumed negligible. Therefore, a Fanno flow approximation was the approach for determining the mass flow rate through each passage. Calculation of the full passage length can be seen in Figure 41 for a 2D approximation.

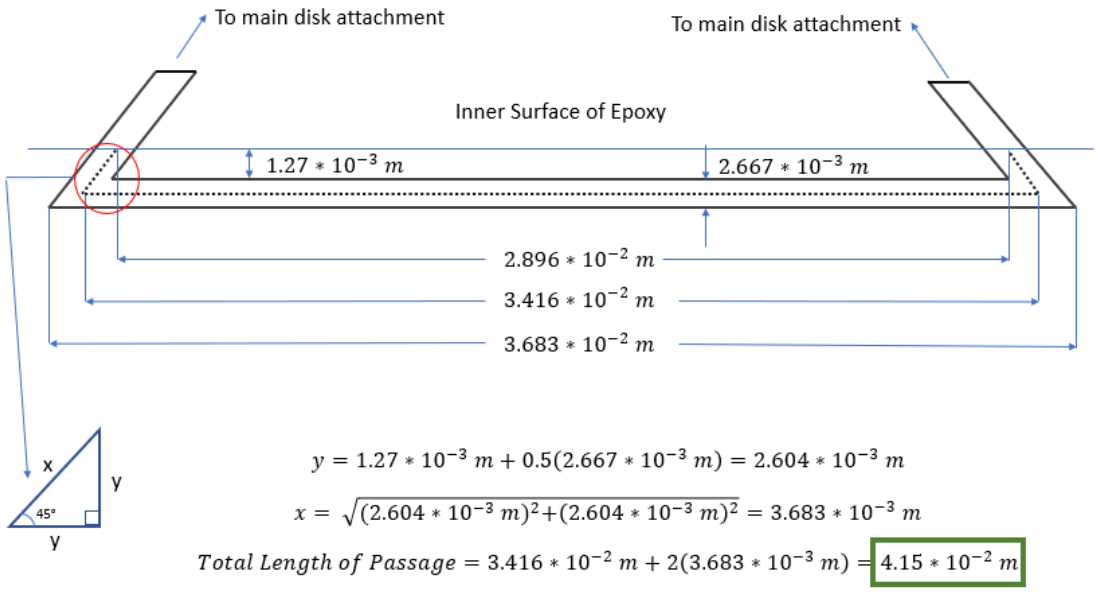

Figure 41. Passage Length Calculation

Calculations were done using Microsoft Excel, and the goal seek function was instrumental in determining the inlet and outlet Mach numbers. These were then used to determine the required number of passages. The calculations were performed in the following manner, and can be seen in full in Appendix C.

Hydraulic diameter of the passage was determined using Equation 1.

$$D_h = \frac{4A}{p} \tag{1}$$

In Equation 1, A is the area and p is the perimeter of the passage cross section. The average layer height of the passage was measured using a portable surface roughness tester to obtain an absolute roughness ε of 8.918E-9m , (3.511E-7in). This provided the ratio of layer height to hydraulic diameter.

$$\frac{\varepsilon}{D_H} = 3.52 * 10^{-6} \tag{2}$$

Dynamic viscosity, density, ratio of specific heats, and the specific gas constant of air were used in the following calculations.

$$\dot{m} = \rho u A = \rho u \frac{\pi D_H^2}{4} = \frac{P}{\sqrt{RT}} AM\sqrt{\gamma} \tag{3}$$

$$R_e = \frac{\rho u D_H}{\mu} = \frac{4\dot{m}}{\pi D_H \mu} \tag{4}$$

$$f \approx \left[-1.8 \log\left[\frac{6.9}{R_e} + \left(\frac{\frac{\varepsilon}{D_H}}{3.7}\right)^{1.11}\right]\right]^{-2} \tag{5}$$

Equation 5 is a correlation between friction factor, Reynold's number, and relative roughness [9]. The mass flow rate was a value calculated using the Mach number at the passage exit, or the injection port. That value was calculated using Fanno flow approximation. Before that could be done, the equivalent length of the pipe had to be determined. In other words, the length of a straight circular pipe that would produce the same losses. Knowing the elbows bent with a radius of 0.00127m, (0.05in) and the flow turned a total of 120° within the pipe, a K factor was estimated as 0.3 using Figure 66 in Appendix D. However, using K factor approximation for a smaller elbow radius would likely have been more appropriate in this case. Equation 6 uses this value to calculate the equivalent length of each elbow bend. This value was doubled and added to the true length of the passage to estimate the equivalent length of the entire passage, L, in Equation 7.

$$Equivalent\ Length = EL = \frac{KD_H}{f} \tag{6}$$

$$L = 2(EL) + \ True\ Passage\ Length \tag{7}$$

The length L was determined to be 0.122m, and was used in the following calculations. The ratio of length to diameter scaled by the friction factor can be used to determine the entering and exit Mach numbers. Note that for previous calculations,

entering Mach number was estimated. The following iterative process was used to determine the actual Mach numbers.

$$\left(\frac{fL}{D_H}\right) = \frac{1-M^2}{\gamma M^2} + \frac{\gamma+1}{2\gamma}\ln\left(\frac{(\gamma+1)M^2}{2\left(1+\frac{\gamma-1}{2}M^2\right)}\right) \tag{8}$$

$$\left(\frac{fL^*}{D_H}\right)_2 = \left(\frac{fL^*}{D_H}\right)_1 - \left(\frac{fL}{D_H}\right)_{1-2} \tag{9}$$

$$\frac{P}{P^*} = \frac{1}{M}\left[\frac{\gamma+1}{2\left(1+\frac{\gamma-1}{2}M^2\right)}\right]^{0.5} \tag{10}$$

Where the term with the subscript 1–2 is solved using the known length, hydraulic diameter, and friction factor, and the other two are related to Mach number using Equation 8. Solving for the Mach number into and out of the passages was done using an iterative approach. With the initial estimate of Mach number into the passage set as 0.5, the Mach number out of the passage was then calculated. Equation 10 was then used to determine the static pressure drop from passage entrance to exit. This pressure drop needed to match the pressure rise measured by Londono in order to determine whether or not the calculated Mach numbers would reflect the actual Mach numbers when tested on this specific engine. The raw data Londono collected in [7] are shown in Figure 42 and Figure 43.

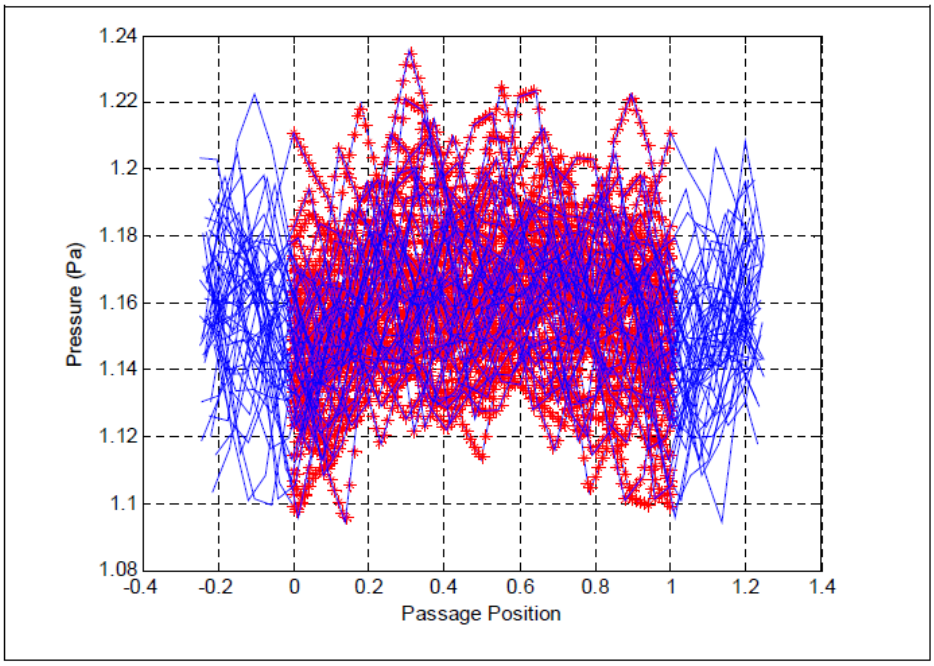

Figure 42. Kulite 7 Pressure Measurements (Bleed Location). Source: [7]

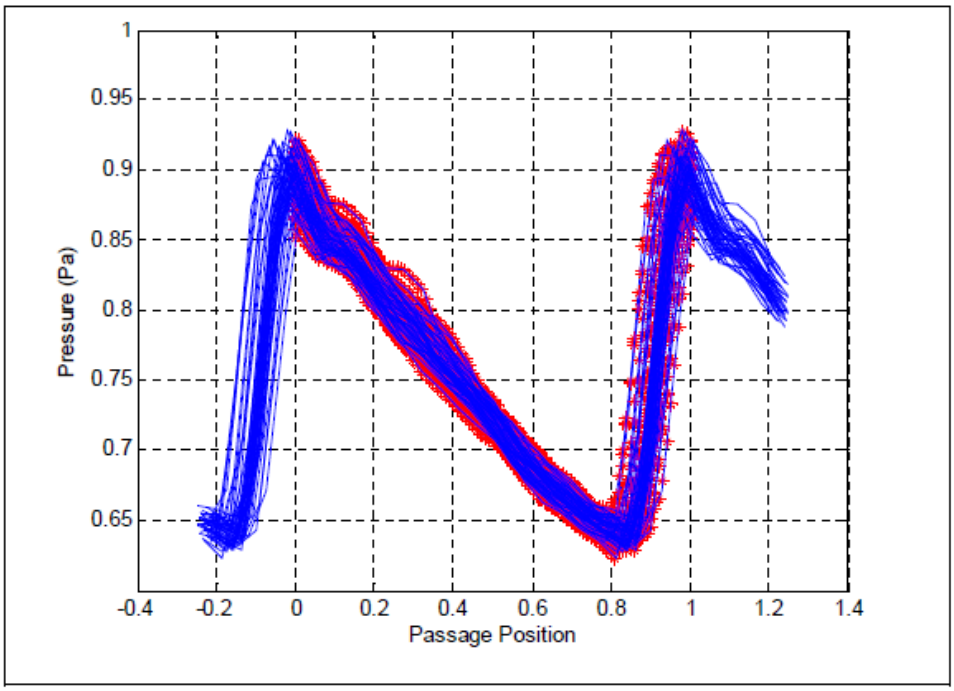

Figure 43. Kulite -1 Pressure Measurements (Injection Location). Source: [7]

The Kulite pressure measurements fore and aft of the blade leading and trailing edges respectively averaged about 0.8 and 1.15 the ambient static pressure. Therefore, the static pressure rise from the location of the bleed to the injection ports was calculated as 1.4375. The pressure drop in the internal passages had to match this value in order to ensure valid results. This was done with the goal seek function in Excel. The pressure rise was sought to be 1.4375, by altering the exit Mach number, and the ratio of length to diameter scaled by the friction factor was determined from that. Goal seek was then used a second time to match that value by altering the entrance Mach number. Once the pressure drop matched and the ratios in Equation 8 matched, the mass flow through a single passage was calculated. Then, depending on what percentage of mass flow recirculation was desired, the number of passages was determined. This resulted in 181 passages for 5.74% recirculation and 89 passages for 2.82% recirculation. Note that the mass flow was originally targeted to be 6% and 3%, but 181 and 89 being prime numbers was a worthwhile change to prevent the disturbance of the passage injection on the rotor blades reaching a resonance frequency and causing damage to the rotor blades.

C. FINAL DESIGNS

Three rings connect the passages to the main disk which positions the system the same way it positioned the surface molds. To create the holes that hold the passage, a single internal passage was patterned in a circle around the ring and the SolidWorks cavity feature was used to subtract the overlapping volume of the passages from the rings. After the cavity had been made, the chamfers on the mold tips were added to provide more clearance for the fitting of passages into the rings. The mold base from the surface treatments was modified to attach the center ring to the main disk, and the rings were held together using the same nuts and bolts as the captured nut systems previously discussed. Figure 44 through Figure 49 show the rings, passages, and many of the same components from the surface treatments. Note that the center ring is in yellow, the side rings are in purple, and the passages are in gray for visualization.

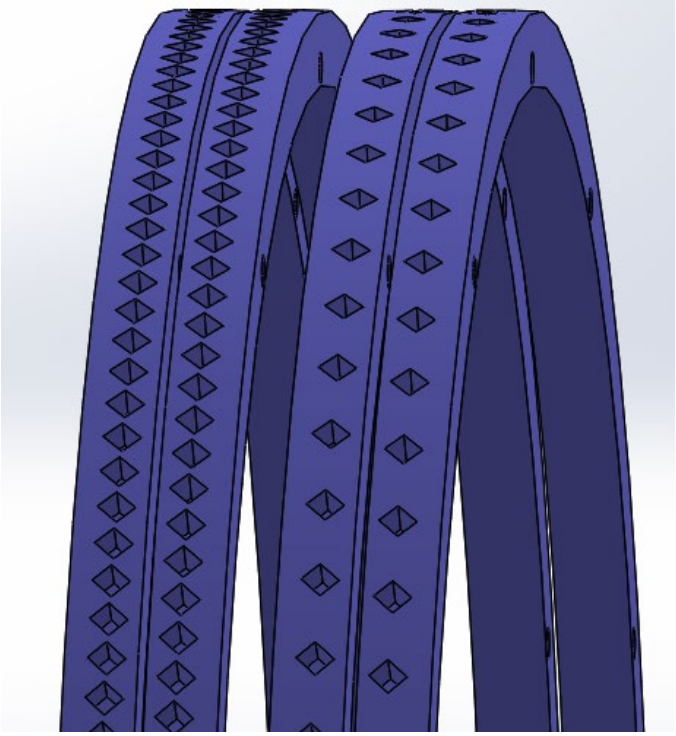

Figure 44. Side Rings for 5.74% and 2.82% Mass Flow Recirculation

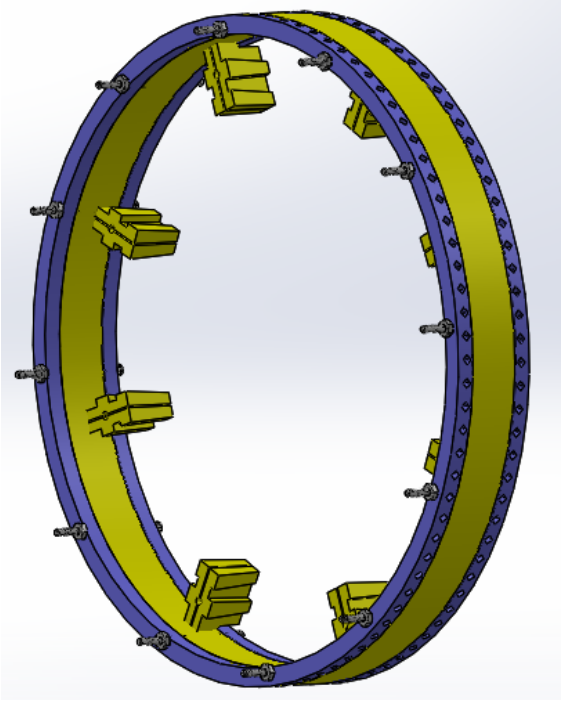

Figure 45. Center and Side Rings

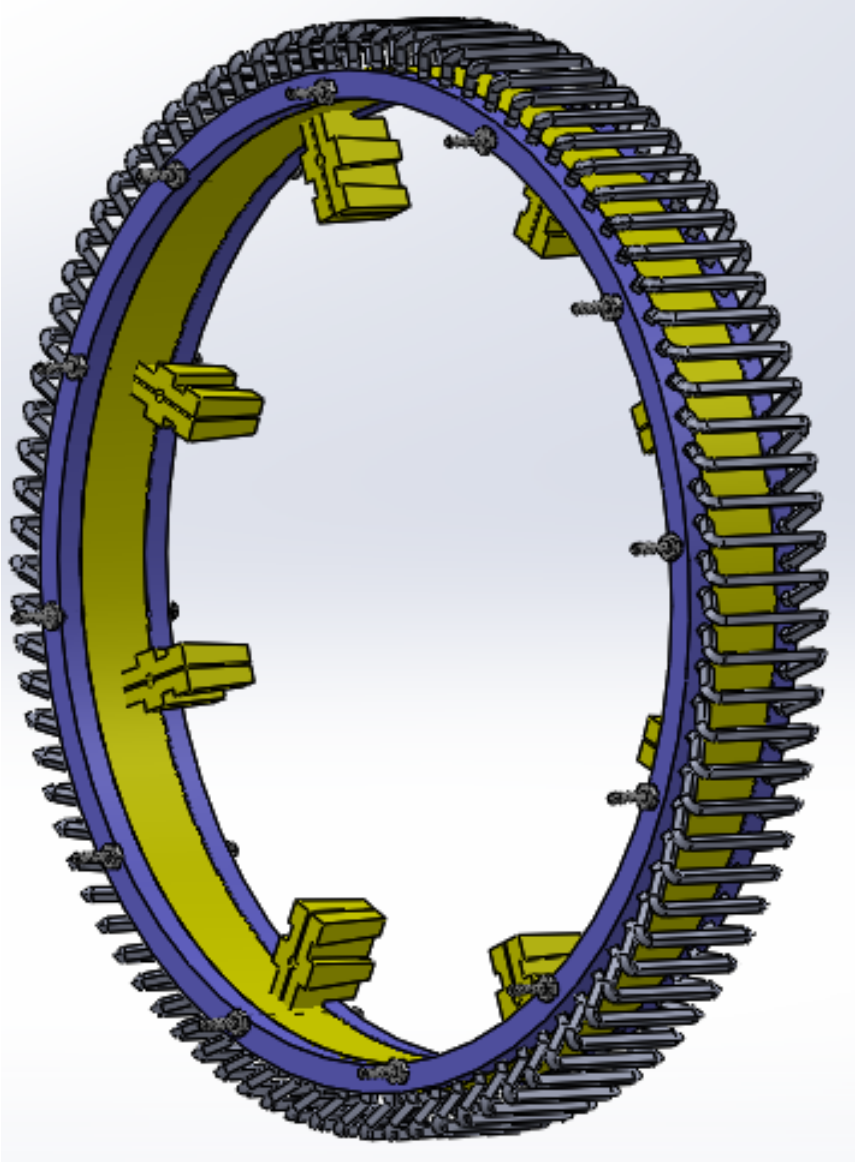

Figure 46. Side Rings, Center Ring, and Internal Passage Molds

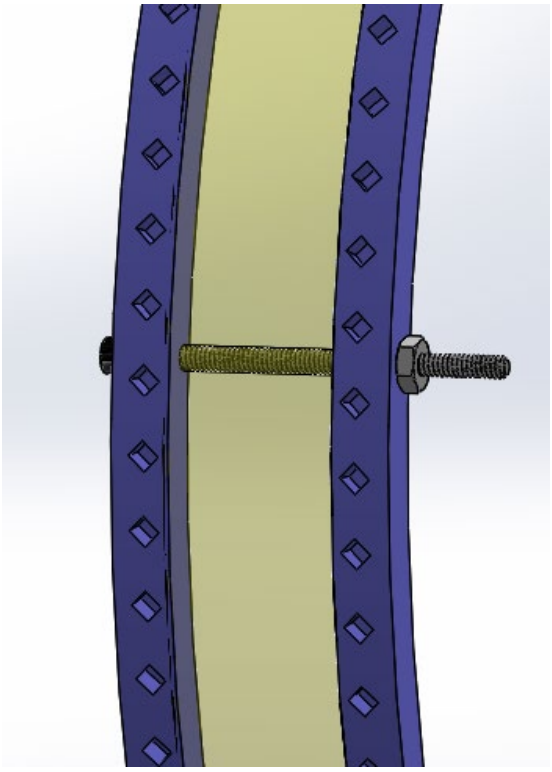

Figure 47. Ring Connection Hardware

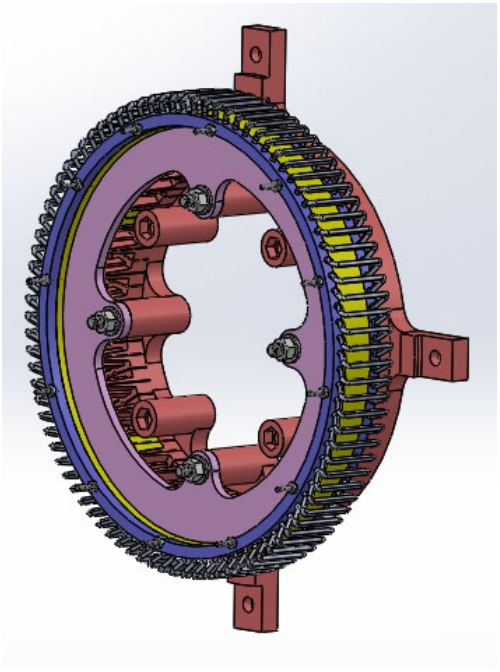

Figure 48. Internal Passage Assembly on the Main Disk

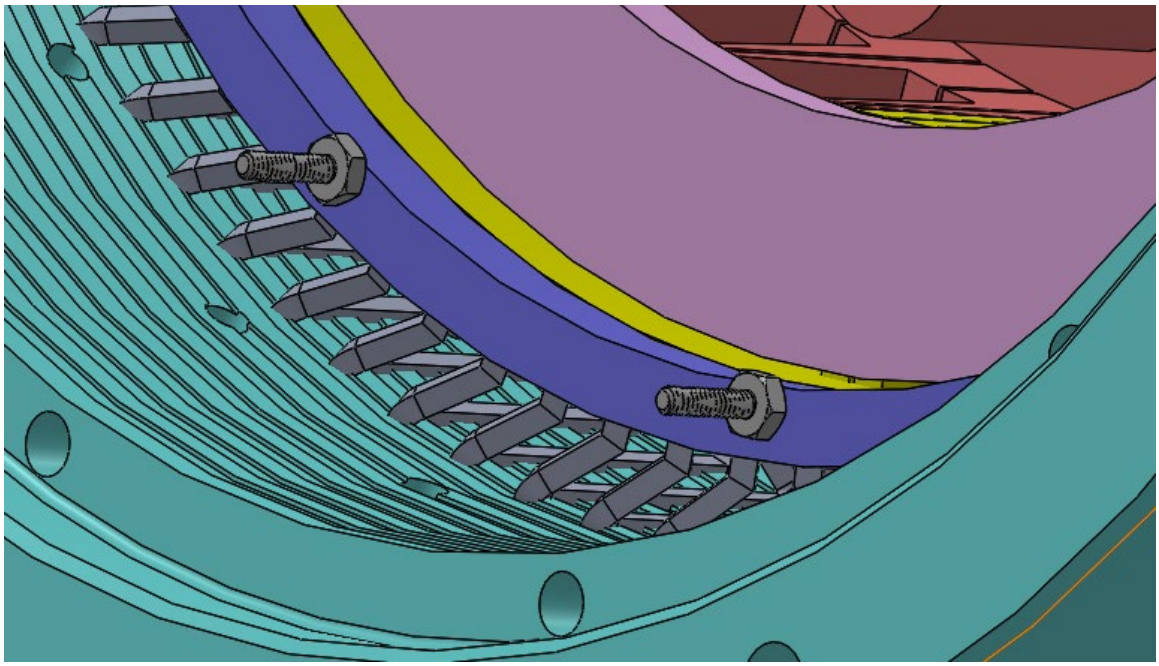

Figure 49. Internal Passages Overlap with the Compressor Casing

To show all of the parts and hardware involved in the internal passage casing treatment process, Figure 50 shows an exploded view of the SolidWorks models.

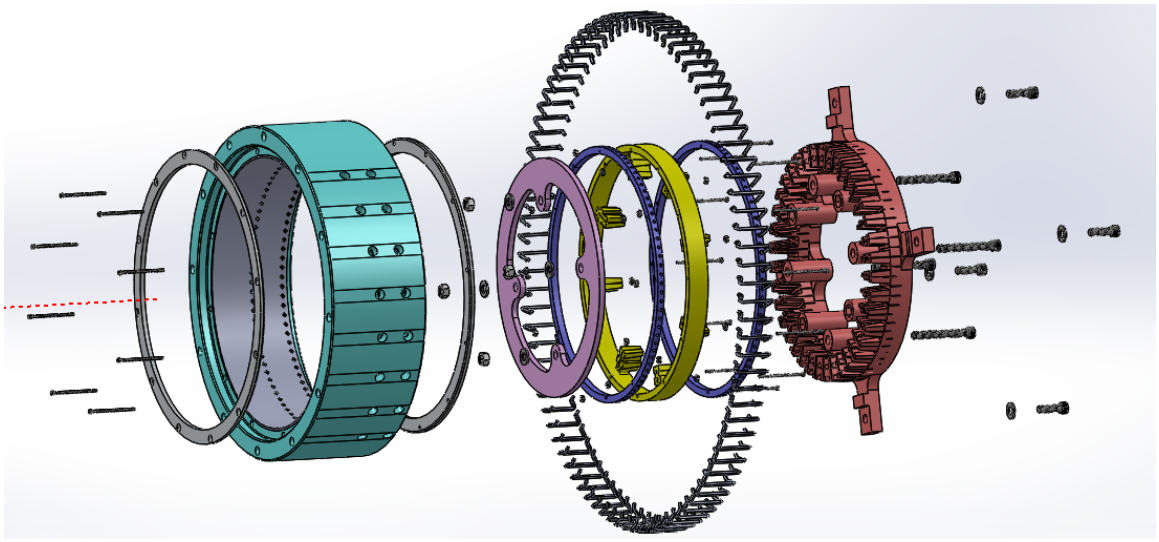

Figure 50. Exploded View of the Internal Passage Casing Treatment Process

Based on the SolidWorks models and knowing that the casing diameter would be increased to allow the passage molds to fit, the resulting cavity should be made after dissolving the molds.

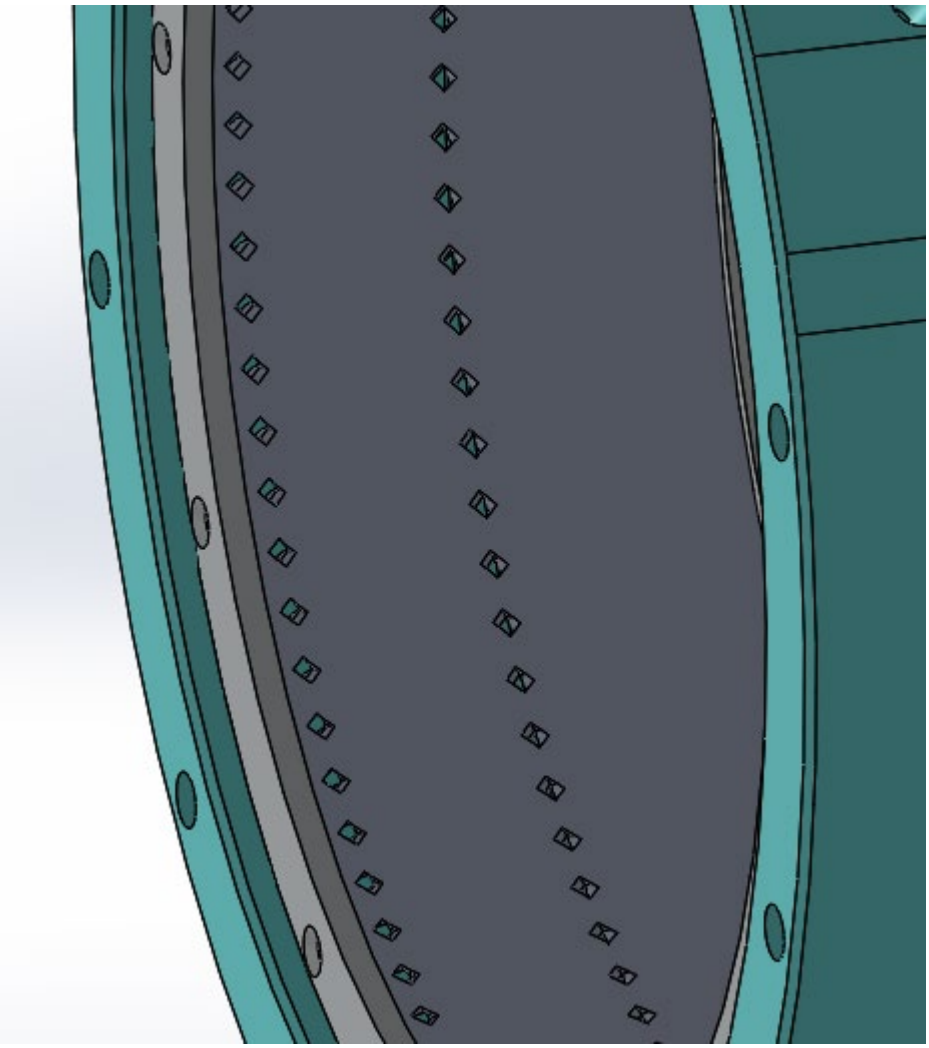

Figure 51. Internal Passages Cast into Epoxy Layer

D. INTERNAL PASSAGE MANUFACTURING PROCESS

The first step of implementing this casing treatment is to attach the two side rings to the center ring via 12 nuts and bolts. Once the system is secure, the internal passages can be placed into the holes in the side rings. The majority of the following steps are the same as the surface treatment process. Therefore, they are described in brief. Next, a

captured nut must be placed in each of the eight t-slot bases and the entire system can be placed on the main disk. However, before placing the passage assembly on the main disk, the casing retaining ring must be placed on first. Then, same retaining disk from the surface treatments can be used to prevent movement in the axial direction. When placing the passages and main disk on the casing, the passages should be pressed all the way to the casing wall.. If the passages are not fitting into the casing, rather than forcing them in, the entire main disk – passage mount system can be cooled to shrink. This was done by placing all plastic components in a refrigerator for approximately 3 hours, causing them to shrink and facilitating their easy assembly into the aluminum casing. Once the temperature returns to room temperature, the plastic expands to its original size and produces a tight fit. The casing wall serves to prevent radial movement of the passage molds while on the lathe. The same process of pouring shown in Figure 11 with the epoxy being set while the casing is spun in a lathe can be used here. The epoxy layup process for the internal passages can be seen in Figure 52 and Figure 53.

Figure 52. Internal Passage System on Lathe

Figure 53. Epoxy Pouring for Internal Passage Treatment

IV. DISCUSSION

A. SURFACE CASING TREATMENTS

The manufacturing process for implementing the surface casing treatment produced the desired geometries in the casing endwall. Figure 54 shows the PVA mold tops stuck in the epoxy layer after the main disk was removed

Figure 54. Compressor Casing Surface Treatment Immediately After Mold Base Removal

Before the molds could be dissolved, the casing had to be sent to be cut to the exact inner diameter needed for the TCR. At the time of writing this thesis the parts were being machined to the final diameter.

The process for implementing the surface treatments has some strong qualities and some drawbacks. The reusable mold bases and easily changed PVA tops make the process easier to repeat or alter for desired geometries. A weakness of the process is that the main disk only allows for a specific number of molds to be made. However, for larger or smaller compressor casings, one of two things would need to change: the molds or the main disk. If the outer diameter of the main disk were able to be increased, more molds may be able to fit on it. With the case of the TCR compressor casing, with molds made of polycarbonate and PVA, only 3.8 molds per rotor blade were able to fit as opposed to 4.0 molds per rotor blade tested by Chen et al. [4]. Nevertheless, when considering the scope of this thesis as creating a process to implement compressor casing treatments, this was a success in that a surface casing treatment manufacturing method was developed that can be tailored to different geometries. Whether or not the casing treatment yields similar results to those achieved in [4] can only be determined by experimental testing.

B. INTERNAL PASSAGES

The manufacturing process for the internal passages also resulted in a completed casing treatment. After the main disk and mounting system were removed from the lathe, all that could be seen extending out form the epoxy were the tips of the PVA passage molds. In order to make machining of the casing to the correct diameter safer for the passages underneath the epoxy surface, the tips were cut off. Figure 55 shows the casing immediately after the epoxy cured, and Figure 56 shows the casing after the main disk was removed but before being machined to the TCR diameter requirement.

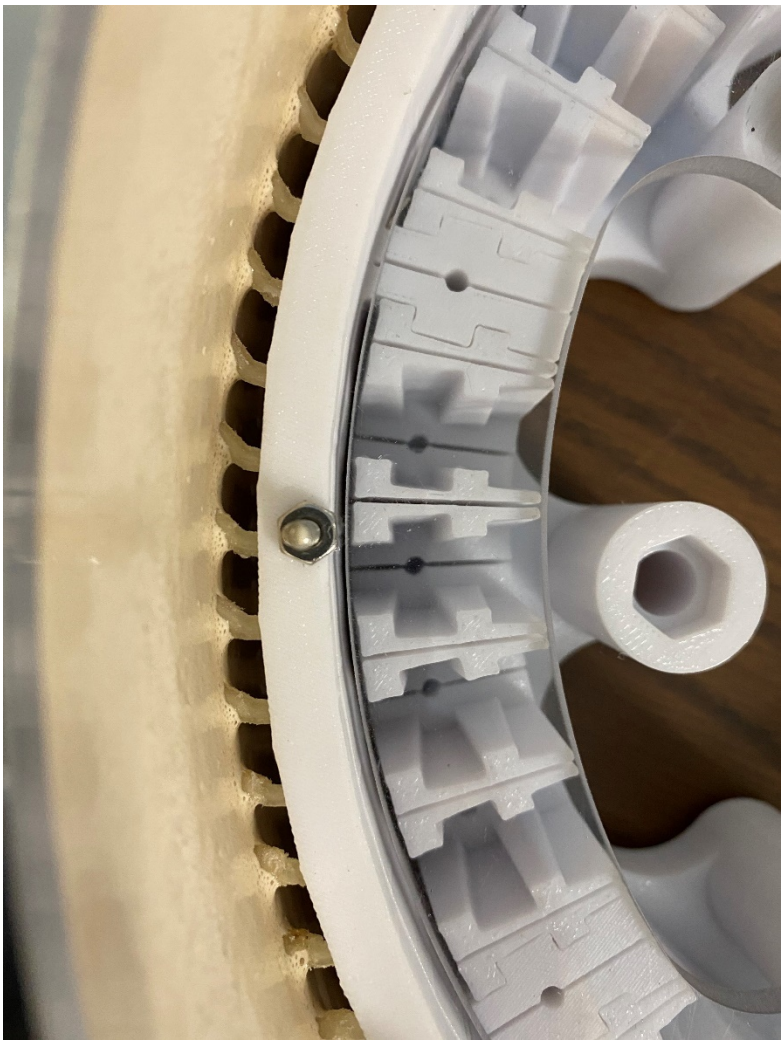

Figure 55. Internal Passage Casing Treatment Immediately After Epoxy Cured

Figure 56. Nearly Completed Internal Passage Casing Treatment

It was important not to machine the casing of either treatment to the required diameter before dissolving the PVA because the molds act as support for the epoxy layer while being machined. Because the internal passages are encased in epoxy, the dissolving time is expected to be much higher than that of the surface treatments. The only way to know for sure if the PVA has completely dissolved will be to run water through each passage and see if water come out the other end. As with the surface casing treatment, at the time of writing this thesis the parts were being machined to their final diameters.

The process for implementing internal passages, while overall successful in producing a casing with the desired number of passages, has some flaws that would need to be addressed for future use. Those changes are addressed in Appendix B. Like the surface treatments, their effectiveness in extending the stability/stall margin of the TCR can only be determined experimentally at a later date. Overall, both manufacturing process successfully implemented casing treatments.

THIS PAGE INTENTIONALLY LEFT BLANK

V. CONCLUSIONS

There were two main findings that stemmed from this thesis. First, it was found that the most successful approach to implementing a surface treatment in epoxy via molds was to use two-piece molds. The tops being made of PVA or some other water-soluble material eliminate the risk of breaking or chipping the epoxy surface upon removal.

For internal passages, it was found that compressible flow with friction calculations can be used to determine how many passages would be needed for a certain mass flow recirculation goal. By determining the entering and exiting Mach numbers to the passages, one could determine the mass flow rate through the passage and therefore how many are needed. By implementing this treatment in the epoxy layer of the casing, the inner diameter only had to be increased by roughly 2% as opposed to recirculating the flow externally.

THIS PAGE INTENTIONALLY LEFT BLANK

APPENDIX A. BILL OF MATERIALS

Item #	Name	Make	Part #	Quantity Used	Price	Purpose	URL
1	18-8 Stainless Steel Socket Head Screw 4-40 Thread Size, 2” Long, Fully Threaded	McMaster Carr	92196A035	38	$9.90 (1 Box of 50)	Use with captured nut (Item #2) to remove disk from molds after epoxy is cured, as well as removing the molds from the epoxy	https://www.mcmaster.com/92196A035/
2	18-8 Stainless Steel Hex Nut 4–40 Thread Size	McMaster Carr	91841A005	39	$3.02 (1 Pack of 100)	Use with Item #1 to remove the main disk from the molds after epoxy is cured, as well as removing the molds from the epoxy	https://www.mcmaster.com/91841A005/
3	18-8 Stainless Steel Socket Head Screw5/16”-18 Thread Size, 1” Long	McMaster Carr	92196A583	4	$10.58 (1 Pack of 25)	Attach main disk to casing	https://www.mcmaster.com/92196A583/
4	Black Oxide Alloy Steel Socket Head Screw 5/16”-24 Thread Size, 2–1/4” Long	McMaster Carr	91251A392	4	$11.74 (1 Pack of 25)	Use with hex nut and washer (Items #5 and #6) to attach retaining disk to main disk	https://www.mcmaster.com/91251A392/
5	18-8 Stainless Steel Hex Nut5/16”-24 Thread Size, MS51972-2	McMaster Carr	90762A123	4	$4.76 (1 Pack of 5)	Use with socket head screw and washer (Items #4 and #6) to attach retaining disk to main disk	https://www.mcmaster.com/90762A123/
6	18-8 Stainless Steel Mil. Spec. Washer, Passivated, 5/16” Screw Size, MS/NASM 15795-812	McMaster Carr	98019A385	8	$6.57 (1 Pack of 25)	Use with socket head screw and hex nut (Items #4 and #5) to attach retaining disk to main disk Can also be used with Item #3	https://www.mcmaster.com/98019A385/
7	Ultimaker Material 1612 PLA Silver Metallic 2.85mm Diameter, 750gram spool	Ultimaker	Varies	1.5	Varies	Printer material used in most test prints	Varies
8	Ultimaker Material PVA 2.85mm Diameter, 750gram spool	Ultimaker	Varies	3	Varies	Printer material used for support material and internal passages	Varies

THIS PAGE INTENTIONALLY LEFT BLANK

APPENDIX B. DESIGN ITERATIONS AND OBSTACLES

The ability to quickly print small test sections of each part was a key factor in identifying design flaws and necessary changes. However, the very nature of how additive manufacturing creates three dimensional objects manifested some challenges of its own and heavily influenced the design of every part. The remainder of this section will describe some of the largest obstacles faced in the design portion of this study so that they may not be made in future studies following this one.

The most prominent consideration that has to be made when designing parts for current additive manufacturing is that the part needs to be able to lie flat on a print bed and be made layer by layer. Therefore, some features that are easily made by subtractive manufacturing, such as overhangs or steep angles, are either not possible or require support material from 3D printers. If a part does require support material, the removal of the support material must then be considered. Some materials such as PVA are water-soluble and are removed quite effortlessly. On the other hand, some need to be picked out with hand tools or the like which can be difficult based on the part geometry. One of the designs for the S-shaped groove molds featured a small hole in the back of the base to be able to push support material out from, shown in the red circle in Figure 57.

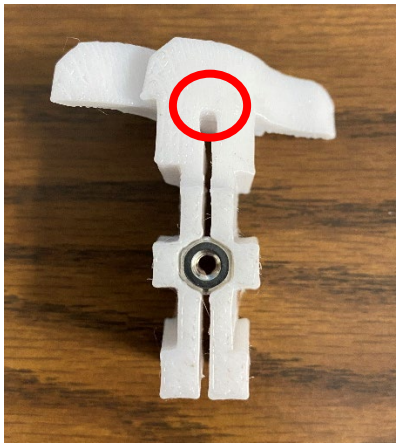

Figure 57. Support Material Removal Aid

The ability of a 3D printer to create the part it is given is not the same across all printers. Fortunately, (at least in the case of this study), a printer can be consistent enough to predict what flaws will occur and make design changes to account for them. Particularly noticeable is the error in dimensions of any given part. For example, initial models of the molds and main disk were unsuccessful when printed because the convex geometries of the molds and slots were printed slightly too large and the concave regions too small. This can be attributed to the actual width of the PLA as it is extruded from the print head. Calipers were used to determine the average error in dimensions and the slots were made that much larger. Figure 58 shows the difference in what was modeled versus what was printed for the slots that hold the molds in place on the main disk.

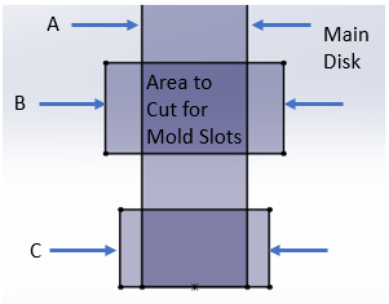

Dimension	Modeled	Printed	Difference
A	0.25	0.2476	-0.0024
B	0.6	0.5950	-0.0075
C	0.4	0.3925	-0.005

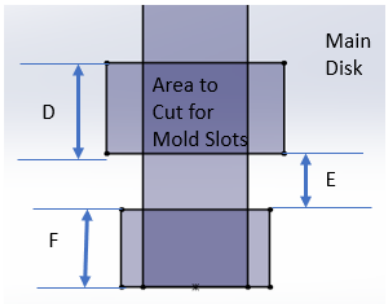

Dimension	Modeled	Printed	Difference
D	0.2	0.1900	-0.01
E	0.3	0.3110	0.011
F	0.2	0.1855	-0.015

Average of all but E: -0.008

Figure 58. Machine Errors in Dimensions for Slots in Main Disk

An opposite trend was observed for the convex dimensions of the molds. In response, the SolidWorks model for the main disk was changed so that there would exist a 2.54E-4m, (0.01in), gap between molds and mold slots. Another solution was to add the previously mentioned slots that allow for elastic deformation of the molds and main disk. These slots combined with the dimension alterations provided successful test prints for the mold and main disk fittings. The final dimensions for the molds and mold slots changed numerous times after these measurements were taken for a number of reasons such as

adding more slots or putting a chamfer on the edges for easier removal. A similar problem occurred when designing the internal passages. The holes in the rings that hold the passages in place were modeled to be the same size as the passage themselves. The difference in this case was that the rings were printed with PLA and the passages with PVA. Instead of measuring out the differences in what was modeled versus what was printed, adding a chamfer to the passage tips solved the issue more elegantly and provided a firm fit.

Another obstacle faced in the design process was 3D printing the internal passages. Because the epoxy layer is so thin, the passages had to be small and a large number of them were required. In order to remove them after the epoxy cured, PVA was the necessary material to print them with. The challenge was that PVA tends to adhere to itself very well, and moving from one tip to the other often caused the part to collapse. This issue was resolved by decreasing the layer height and print speed, and increasing the cooling fan speed. This reduced the amount of PVA being extruded at a time and cooled it faster so that it would harden before the print head moved to the next tip. Another issue that arose with the internal passages was PVA rolling up and adhering to the extruding nozzle. The clumped and burnt material had to be scraped and picked off of the nozzle after each print, and limited the number of passages that could be printed at one time to ten. Trying to print more than ten passages at a time consistently caused failed prints due to the nozzle build-up. An example of PVA build-up on the nozzle can be seen in Figure 59.

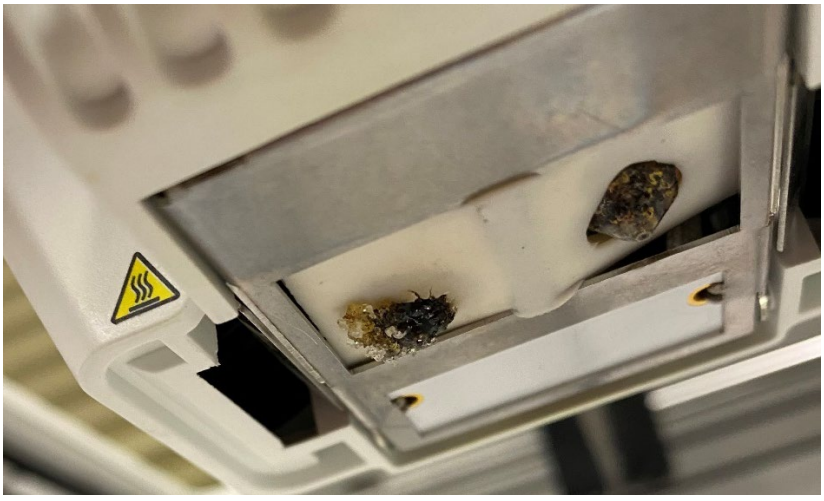

Figure 59. PVA Build-up on the Printcore Nozzle

This was somewhat a temporary fix to an underlying issue with the passage geometry. An estimated 20% of the passages attempted to print failed before completing. The ones that did complete had very rough edges that needed to be sanded down by hand. It is recommended that the tips be made larger or of different shape to attach to the mounting rings. This would, however, require similar alterations to the mounting itself. If such alterations were made, it is recommended that the passages be somehow clamped to the mounts rather than pushed in the way they are now. Inserting the passage molds into the rings was also a tedious task that saw several molds break.

A consideration to make when working with epoxy is the inclusion of thin segments. In other words, it is important not to design a part that will create chips of epoxy that would chip off or break under loads. This was a concern for both the surface treatments and the internal passages. Figure 60 illustrates this situation.

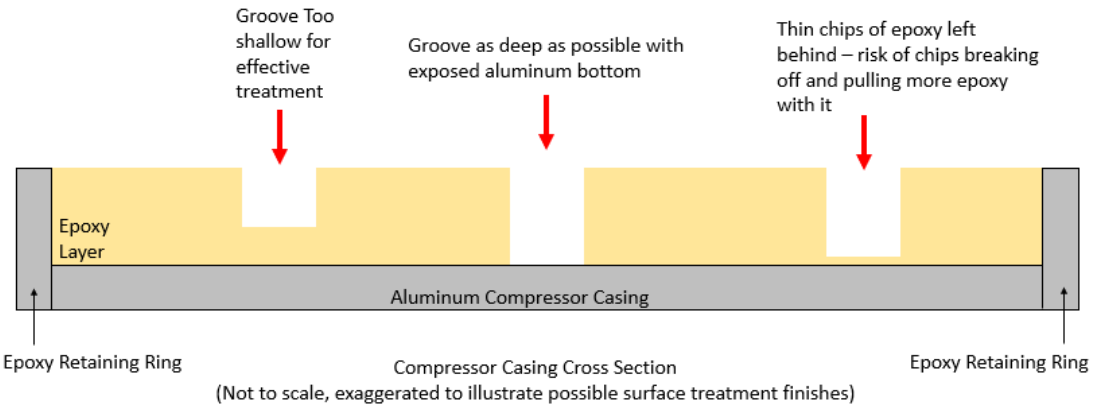

Figure 60. Epoxy Finish Including Thin Chips

The final design for the surface treatments was to have the molds extend all the way to the top of the grooves in the aluminum casing. However, a decision was made to machine out the grooves in order to allow for deeper treatments. The target was the center situation in Figure 60, leaving behind no thin chips and providing as deep a treatment as possible.

Unless they are made of PVA, single piece molds have to be pulled out of the epoxy radially. If future molds are made as a single piece, a mold release agent must be used to

ensure a proper finish is cast into the epoxy. Three release agents were tested by spraying molds and placing them in small batches of epoxy. When cured, the molds were removed with pliers, and the ease of removal and finish of the cast was considered. The release agents one should consider using would vary based on the material the mold is made of and the interaction with the epoxy. Figure 61 and Figure 62 demonstrate the method of testing release agents.

Figure 61. Testing Mold Release Agents

Figure 62. S-Grooves Cast from Epoxy Test

Some of the tests had favorable results in that the epoxy was well intact and there was a smooth finish. However, many of the casts resulted in chips broken from the epoxy surface, especially between the neighboring S-grooves. Knowing that 38 molds would need to be removed without surface flaws lead to the decision to print the molds as two parts. The tops would be sacrificial PVA, and the bases would be reusable polycarbonate. This eliminated the need to pull anything out of the epoxy by force.

The U-shaped grooves were designed with many of the same considerations as the S-shaped grooves. However, because the U-shaped grooves do not have overlapping inlets and outlets, they had to be shortened in the circumferential direction. In addition, the swept corners on the front and rear of the mold base seen on the S-shaped molds were not needed for the U-shaped molds. Because the inlets and outlets of the S-shaped grooves overlap, the base needed to be cut in order to allow for the insertion of the molds in the main disk. The U-shaped grooves were not printed or tested in this study, only designed in SolidWorks

as a single unit as opposed to having a PVA top like the S-shaped molds, and can be seen in Figure 63.

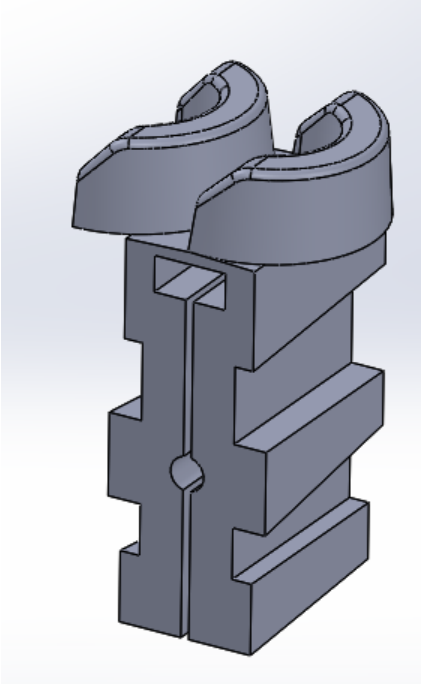

Figure 63. U-Shaped Groove Mold

The removal of the U-shaped molds, (or any single piece mold), would rely on another captured nut, this time in the radial direction. Another 3D printed part, named the puller tool, could be used with a nut and bolt to pull the molds out from the epoxy. Figure 64 shows the radial captured nut system.

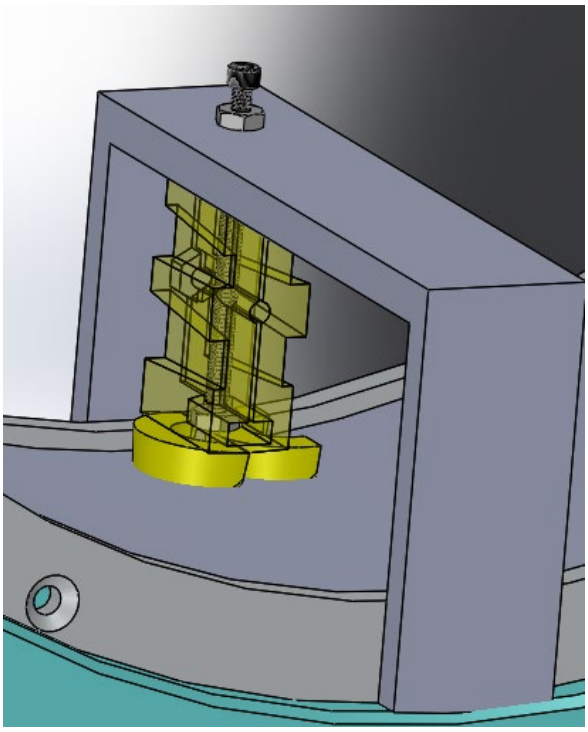

Figure 64. Radial Captured Nut System for a Single Piece Mold

Here, the captured nut in the mold base is held in place by the shape of the hole it rests in. The bolt, (with the second nut at the top already in place), is tightened to the captured nut and then held in place while the top nut is turned. The top nut pushes the bolt off of the puller tool, and the bolt pulls the captured nut, (and therefore the mold), out of the epoxy. While this method was not tested for the U-shape grooves experimentally, it proved to work for the S-shape groove molds in that it pulled the molds out. The method was not used for the S-grooves as already mentioned, but may still be useful for molds of other geometries.

APPENDIX C. FANNO FLOW CALCULATIONS

A. CALCULATIONS

$$Actual\ Length = 0.0415m$$

$$Circumferential\ Side = \ 0.002413m$$

$$Radial\ Side = 0.002667m$$

$$A = 6.4358 * 10^{-6}m^2$$

$$p = 2(Radial\ Side) + 2(Circumferential\ Side) = 0.0102m$$

$$D_h = \frac{4A}{p} = 0.0025m$$

$$\varepsilon = 8.9179 * 10^{-9}m$$

$$\frac{\varepsilon}{D_h} = 3.5198 * 10^{-6}$$

(The following equations represent the iterative portion of calculations. They were initialized by estimating a Mach number into the passage inlet and a static pressure and temperature. The final values are listed here.)

$$\dot{m} = \rho u A = \rho u \frac{\pi D_H^2}{4}$$
$$(estimated\ to\ initialize\ Reynold's\ number)$$

$$R_e = \frac{\rho u D_H}{\mu} = \frac{4\dot{m}}{\pi D_H \mu} = 7.48 * 10^4$$

$$f \approx \left[-1.8 \log\left[\frac{6.9}{R_e} + \left(\frac{\frac{\varepsilon}{D_H}}{3.7}\right)^{1.11}\right]\right]^{-2} = 0.019$$

$$K = 0.3$$

$$EL = \frac{KD_H}{f} = 0.0401m$$

$$L = 2(EL) + Actual\ Length = 0.1217m$$

$$\left(\frac{fL}{D_H}\right)_{1-2} = 0.019 * \frac{0.1217m}{0.0025m} = 0.911$$

$$\left(\frac{fL^*}{D_H}\right)_2 = \left(\frac{fL^*}{D_H}\right)_1 - \left(\frac{fL}{D_H}\right)_{1-2}$$

$$\left(\frac{fL}{D_H}\right) = \frac{1-M^2}{\gamma M^2} + \frac{\gamma+1}{2\gamma}\ln\left(\frac{(\gamma+1)M^2}{2\left(1+\frac{\gamma-1}{2}M^2\right)}\right)$$

(Iterations used goal seek to find entering and exiting Mach numbers)

$$M_1 = 0.4926$$
$$M_2 = 0.6927$$

$$\frac{P}{P^*} = \frac{1}{M}\left[\frac{\gamma+1}{2\left(1+\frac{\gamma-1}{2}M^2\right)}\right]^{0.5}$$

$$\frac{P_1}{P_2} = \frac{P_1}{P^*}\frac{P^*}{P_2}$$

$$\dot{m} = \frac{P}{\sqrt{RT}}AM\sqrt{\gamma} = 0.0026618\frac{kg}{s}$$

Where:

$$P = \frac{1}{1.4375}(1.15)(P_{amb}) = 167.75kPa$$

And:

$$M_{compressor} = 1.29$$

$$T_0 = T_{amb}\left(1+\frac{\gamma-1}{2}M^2_{compressor}\right) = 283.85K$$

$$T = \frac{T_0}{1+\frac{\gamma-1}{2}M_2^2} = 350.24K$$

(P_{amb} of 101.37kPa and T_{amb} of 288K)

$$number\ of\ passages = N$$

$$N_{3\%} = 89\ N_{6\%} = 181$$

$$\dot{m}_{recirculated} = \dot{m}(N) = 0.2369\frac{kg}{s}, 0.4818\frac{kg}{s}$$

$$\dot{m}_{compressor} = 8.4\frac{kg}{s}$$

$$\%recirculated = \frac{\dot{m}_{recirculated}}{\dot{m}_{compressor}} * 100\% = 2.82\%, 5.74\%$$

B. ITERATION PROCESS IN EXCEL

Step 1: Seek $\frac{P_1}{P_2}$ to equal 1.4375 by changing the exit Mach number. This will change the reference $\left(\frac{fL^*}{D_H}\right)_2$.

Step 2: Seek $\left(\frac{fL^*}{D_H}\right)_2$ to be equal to the reference $\left(\frac{fL^*}{D_H}\right)_2$ by changing the entering Mach number. This will change the value of $\frac{P_1}{P_2}$. Repeat until $\frac{P_1}{P_2}$ is 1.4375 and $\left(\frac{fL^*}{D_H}\right)_2$ equals the reference $\left(\frac{fL^*}{D_H}\right)_2$.

THIS PAGE INTENTIONALLY LEFT BLANK

APPENDIX D. TABLES AND CHARTS

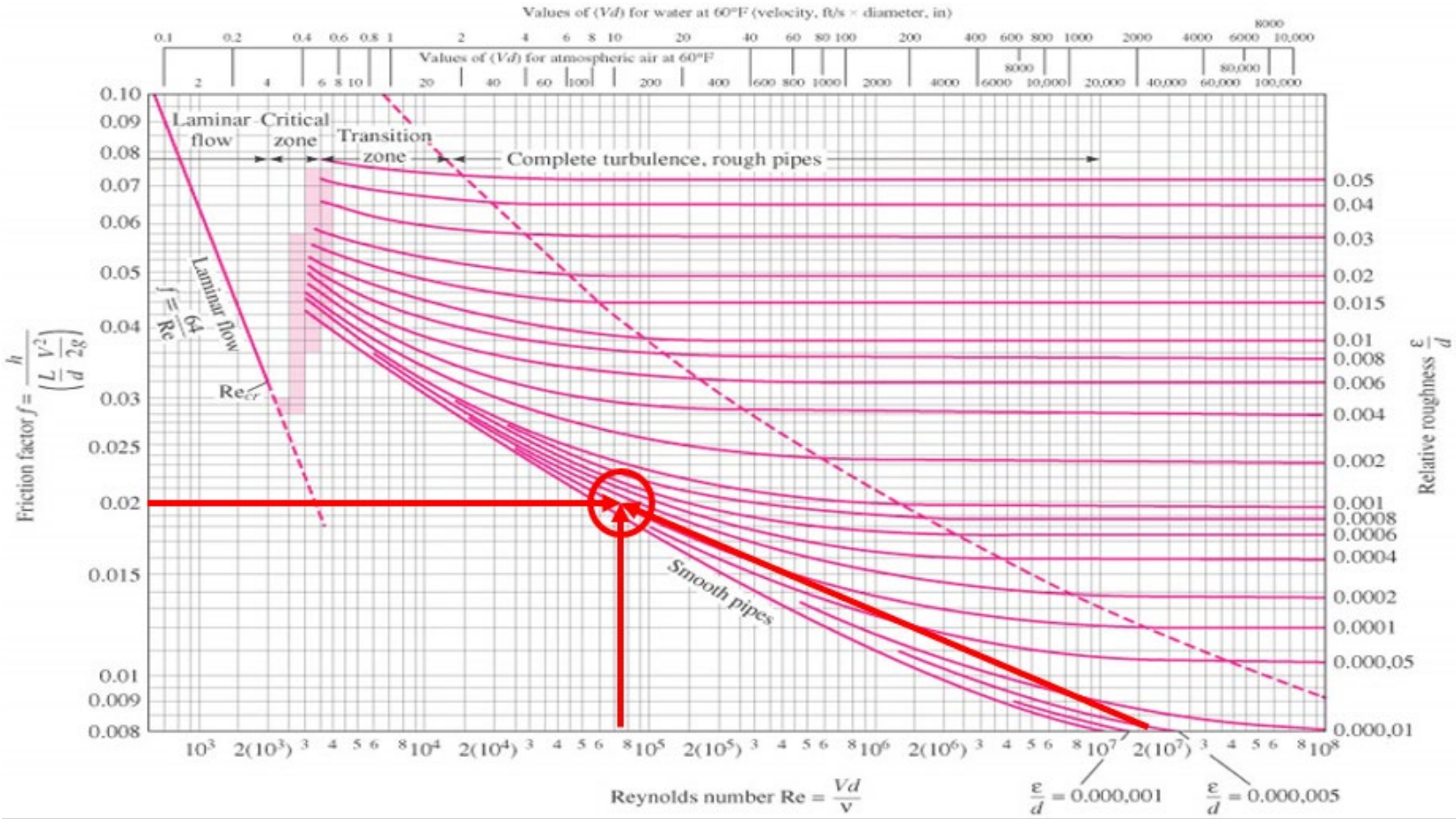

Figure 65. Moody Diagram. Source: [9]

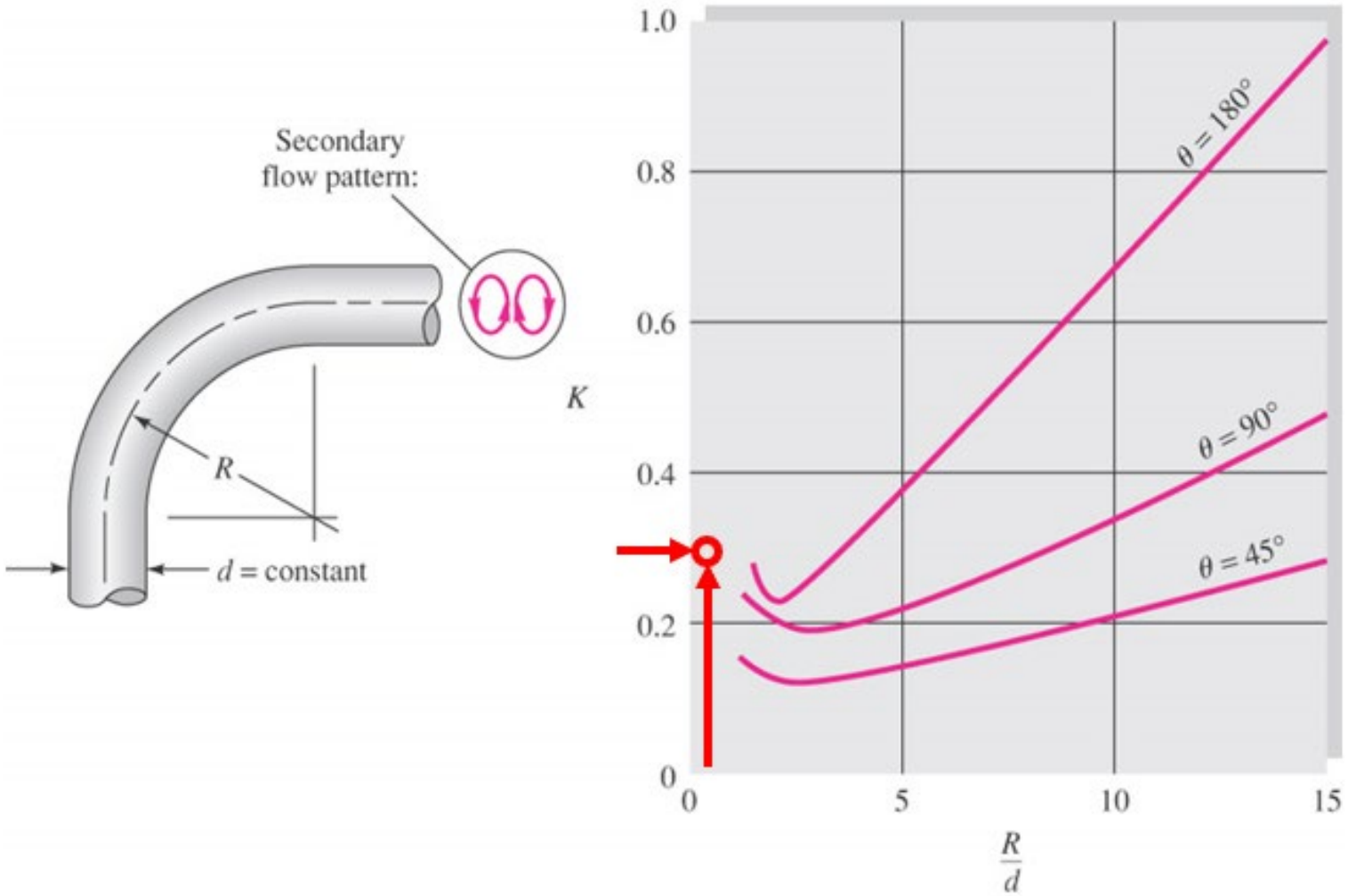

Figure 66. Resistance Coefficient for Bends in Pipes. Source: [9]

LIST OF REFERENCES

[1] "Gas Turbine Parts" [Online]. Available: https://www.grc.nasa.gov/www/k-12/VirtualAero/BottleRocket/airplane/turbparts.html. [Accessed: 26-May-2021].

[2] Furukawa, M., Inoue, M., Saiki, K., and Yamada, K., 1998, "The Role of Tip Leakage Vortex Breakdown in Compressor Rotor Aerodynamics," GT1998, Volume 1: Turbomachinery.

[3] Li, Y., Chen, H., Tan, D., and Katz, J., 2019, "On the Effects of Tip Clearance and Operating Condition on the Flow Structures Within an Axial Turbomachine Rotor Passage," Journal of Turbomachinery, 141(111002).

[4] Chen, H., Koley, S. S., Li, Y., and Katz, J., 2019, "Systematic Experimental Evaluations Aimed at Optimizing the Geometry of Axial Casing Groove in a Compressor," GT2019, Volume 2A: Turbomachinery.

[5] Chen, H., Li, Y., Shankha Koley, S., and Katz, J., 2020, "Effects of Axial Casing Grooves on the Structure of Turbulence in the Tip Region of an Axial Turbomachine Rotor," GT2020, Volume 1: Aircraft Engine; Fans and Blowers.

[6] Hathaway, M. D., 2007, "Passive Endwall Treatments for Enhancing Stability," NASA Techincal Rep., NASA/TM-20.

[7] Hathaway, M. D., 2002, "Self-Recirculating Casing Treatment Concept for Enhanced Compressor Performance," *GT2002*, Volume 5: Turbo Expo 2002, Parts A and B, pp. 411–420.

[8] Londono, Andrea., 2011, *Near-Stall Modal Disturbances within a Transonic Compressor Rotor*, Calhoun.

[9] White, F. M., 2008, *Fluid Mechanics*, 6th ed., McGraw-Hill, New York, NY, Chap. 6.

THIS PAGE INTENTIONALLY LEFT BLANK

INITIAL DISTRIBUTION LIST

1. Defense Technical Information Center
   Ft. Belvoir, Virginia

2. Dudley Knox Library
   Naval Postgraduate School
   Monterey, California